An inducible genome editing system for plants

Xin Wang[1,2], Lingling Ye[1,2,4], Munan Lyu[1,2,4], Robertas Ursache[3,4], Ari Löytynoja[1], Ari Pekka Mähönen[1,2,*]

1. Institute of Biotechnology, HiLIFE, University of Helsinki, Helsinki 00014, Finland
2. Organismal and Evolutionary Biology Research Programme, Faculty of Biological and Environmental Sciences, and Viikki Plant Science Centre, University of Helsinki, Helsinki 00014, Finland
3. Department of Plant Molecular Biology, Biophore, Campus UNIL-Sorge, University of Lausanne CH-1015, Lausanne, Switzerland
4. These authors contributed equally.

*Author for correspondence: AriPekka.Mahonen@helsinki.fi

ORCID IDs: 0000-0002-8982-9848 (X.W.), 0000-0003-3834-862X (L.Y.), 0000-0003-1645-3488 (M.L.), 0000-0002-3803-253X (R.U.), 0000-0001-5389-6611 (A.L.), 0000-0001-6051-866X (A.P.M.)

ABSTRACT

Conditional manipulation of gene expression is a key approach to investigating the primary function of a gene in a biological process. While conditional and cell-type specific overexpression systems exist for plants, there are currently no systems available to disable a gene completely and conditionally. Here, we present a novel tool with which target genes can be efficiently conditionally knocked out by genome editing at any developmental stage. Target genes can also be knocked-out in a cell-type specific manner. Our tool is easy to construct and will be particularly useful for studying genes which have null-alleles that are non-viable or show pleiotropic developmental defects.

MAIN TEXT

Studies of gene function typically rely on phenotypic analysis of loss-of-function mutants. However, mutations may lead to gametophytic or embryonic lethality, or early developmental defects, impeding studies in postembryonic plants. The genome of the model species *Arabidopsis* contains a substantial number of such essential genes, though the precise number remains unknown[1]. Developing a tool that enables conditional and cell-type specific gene disruption is therefore of great value for comprehensively investigating gene function in specific developmental or physiological processes.

Different strategies have been pursued for this purpose. One widely applied approach is the inducible expression of silencing small RNAs[2,3]. However, this results in only a partial reduction of transcript levels, which may hinder a full investigation of gene function. Furthermore, since small RNAs can be mobile[4], constraining the knockdown effect to a given cell-type is challenging. These limitations can be overcome by using the Cre/lox based clonal deletion system[5-7], or Zinc finger nuclease[8] (ZFN) and transcription activator-like effector nuclease[9] (TALEN) based gene editing systems, which provide the possibility of a conditional generation of full knockout. However, these methods rely on complicated genetic engineering and have thus remained rather marginal techniques.

The CRISPR-Cas9 system consists of components derived from the prokaryote adaptive immune system which have been modified for use as a genome editing toolkit in eukaryotes. The endonuclease activity of Cas9 produces double-strand breaks (DSB) in DNA when directed to a target by a single guide RNA (sgRNA). The subsequent error-prone DSB repair mediated by non-homologous end joining facilitates knockout generation. Thus far, CRISPR-Cas9 has been used in plants to generate stable knockouts[10] and somatic knockouts at fixed developmental stages by driving Cas9 expression with tissue-specific promoters[11]. By integrating the well-established

CRISPR-Cas9 technology[12] with an XVE-based cell-type specific inducible system[13,14], we developed an Inducible Genome Editing (IGE) system in *Arabidopsis* which enables efficient generation of target gene knockouts in desired cell types and at desired times.

To achieve this, we first generated a fusion of a small nucleolar RNA promoter[12] and an sgRNA (*pAtU3/6-sgRNA*) in two sequential PCR amplification steps (Fig. 1a). The fusion was then cloned into the *p2PR3-Bsa I-ccdB-Bsa I* entry vector (3rd box) by Golden Gate cloning[12]. This method allows simultaneous cloning of several *pAtU3/6-sgRNA* fragments, if needed. Next, we recombined a plant-codon optimized *Cas9p*[12] into *pDONR 221z* (2nd box). Finally, the IGE binary vector was generated in a single MultiSite Gateway LR reaction by combining an estrogen-inducible promoter (1st box), *Cas9p* (2nd box), *pAtU3/6-sgRNA* (3rd box) and a plant-compatible destination vector[13,15] (Fig. 1a). To facilitate screening of transformed seeds, we also generated two non-destructive fluorescent screening vectors (Extended Data Fig. 1). The availability of a large collection of cell-type specific or ubiquitous inducible promoters[13] and of destination vectors with different selection markers[13,15] makes the IGE system quite versatile. In summary, an IGE construct can be generated in two cloning steps: first, generating a *pAtU3/6-sgRNA* entry vector by Golden Gate cloning and then performing an LR reaction.

Next, we tested the IGE system in the *Arabidopsis* root meristem (RM) by targeting well-established regulatory genes that are essential for RM development. In the RM, a subset of AP2/EREBP family transcription factors, including *PLETHORA1* (*PLT1*) and *PLT2*, form gradients with maxima at the quiescent center (QC) to drive the transition from stem cells to differentiated cells[16-18]. The double mutant *plt1,2* exhibits a fully differentiated RM 6-8 days after germination[16], which can be rescued by complementing it with *gPLT2-3xYFP*[18]. The fused 3xYFP restricts the mobility of PLT2[18], making it possible to observe cell-specific effects of editing *PLT2* (Fig. 1c). We designed four sgRNAs to target *PLT2* in the *gPLT2-3xYFP*; *plt1,2*[18] background (Supplementary Fig. 1). *Cas9p* or nuclease-dead *Cas9p* (*dCas9p)* were transcribed under the inducible, broadly-

expressed promoter *35S:XVE* (*ip35S*)[13]. While induction of *dCas9p* had no effect on PLT2-3xYFP levels (Fig. 1d), *Cas9p* induction led to a weakening of the YFP signal almost in every transformant (Fig. 1e). YFP fluorescence was initially reduced in the root cap and occasionally in the epidermis or stele. Prolonged induction gradually abolished the YFP signal and led to RM differentiation after 8-10 days of induction (Fig. 1e and Supplementary Table 1), similar to the uncomplemented *plt1,2* mutant[16]. The disappearance of YFP fluorescence and subsequent appearance of RM differentiation phenotype suggests IGE-mediated genome editing efficiently disabled PLT2.

Next, we investigated whether the IGE system can be used to induce removal of PLT2-3xYFP fluorescence in a cell-type specific manner. We tested four inducible promoters: *pWOL:XVE* (*ipWOL*), *pWOX5:XVE* (*ipWOX5*), *pSCR:XVE* (*ipSCR*), and *pWER:XVE* (*ipWER*)[13], the expression of which, together, covers most of the cell types in the RM. *Cas9p-tagRFP* was used to monitor promoter activity. Constructs were transformed into *gPLT2-3xYFP*; *plt1,2*. Along with promoter-specific Cas9p-tagRFP expression, we observed a corresponding dampening of the YFP signal in the respective domains after one day of induction (Fig. 2a). We noticed that inducible YFP dampening capability is stably transmitted to the T2 generation (Supplementary Fig. 2), demonstrating that the IGE system can be repetitively used in subsequent generations. Consistent with the role of *PLT2* in promoting stem cell maintenance and QC specification, inducing *Cas9p* in promoter-specific tissues caused premature cell expansion or differentiation of the endodermis, QC, or epidermis/lateral root cap (LRC) after 3 days of induction (Fig. 2b). This reflects the cell-autonomous function of *PLT2* in maintaining an undifferentiated cell state. In addition to QC differentiation, we observed a shift in *ipWOX5* promoter activity towards the provasculature, which resulted in a larger area lacking the YFP signal (Fig. 2b; left panel in *ipWOX5*). The QC and adjacent provascular cells gained columella cell identity, as revealed by the accumulation of starch granules (Fig. 2b; right panels in *ipWOX5*). These results indicate that new QC cells were re-specified from provascular cells following differentiation of the original QC, and the consequent re-

specification and differentiation of the QC gradually led to a larger domain without YFP. These results are consistent with experiments in which laser ablation of the QC leads to re-specification of a new QC from provascular cells[19].

We found that loss of YFP fluorescence correlates strongly with the expression level, the expression region and the timing of induction of Cas9p-tagRFP (Supplementary Fig. 3 and Extended Data Fig. 2). To demonstrate that the loss of YFP fluorescence was due to IGE-mediated *PLT2* editing, we first performed genotyping analysis with intact root samples. Using primers spanning all four targets, PCR detected a strong truncated band in pooled T1 transformants after Cas9p induction. The size of the band corresponds to fragment deletion between targets of sgRNA1 and sgRNA4, which was further confirmed by Sanger sequencing (Supplementary Fig. 4). Next, we isolated Cas9p-tagRFP and YFP-only cells by fluorescence-activated cell sorting (FACS) to compare genome editing efficiency between these two cell populations. The same truncated band was more prevalent in RFP-positive cells than in YFP-only cells (Supplementary Fig. 5a and Extended Data Fig. 3a). Quantitative PCR analysis estimated that the large fragment deletion efficiency in RFP-positive cells is 59-73% (Extended Data Fig. 3b, 3c). In addition to the large deletions, we also identified small indels predominantly in Cas9p-tagRFP positive cells, especially at the target sites of sgRNA1 and sgRNA4 through TIDE (Tracking of Indels by DEcomposition)[20] analysis (Supplementary Data 1). When driving sgRNA1 expression under different promoters, we found that *AtU3b* and *AtU6-29* were the most efficient promoters, at least in the *Arabidopsis* RM (Extended Data Fig. 4 and Supplementary Table 1), thus explaining why sgRNA1 (driven under *AtU3b*) and sgRNA4 (driven under *AtU6-29*) targets were most efficiently edited. Interestingly, already after 8h induction, before visible YFP signal decrease, Cas9p-RFP positive cells displayed 52-70% deletion efficiency, indicating that genome editing in vivo is a fast process (Supplementary Fig. 5b, Extended Data Fig. 2, 3c and Supplementary Data 1). We also constructed IGE-PLT2 lines with only single sgRNA. Both TIDE analysis and amplicon deep sequencing showed markedly

124 higher indel mutation frequency of *PLT2* in Cas9p-tagRFP positive cells than in YFP-only cells
125 (Supplementary Fig. 6 and Supplementary Data 2). In conclusion, IGE-PLT2 enables efficient
126 PLT2-3xYFP mutation, and the loss of fluorescence after Cas9p induction can be used as reliable
127 indicator of target gene mutation.

128 To test whether the IGE system can edit other loci, we targeted a key gene encoding a cell cycle
129 regulator, *RETINOBLASTOMA-RELATED* (*RBR*)[7,21]. The *RBR* null allele is gametophyte-lethal[21].
130 Previous conditional knockdown and clonal deletion experiments have shown that RBR has a role
131 in restricting stem cell division in the RM[6,7,22]. IGE-RBR constructs were transformed into a
132 background in which *RBR-YFP* complements an *RBR* artificial microRNA line, *35S:amiGORBR*
133 (*amiGORBR*)[22]. After one day of induction, we observed loss of YFP specifically in the respective
134 promoter domains (Fig. 2c). Three days of induction led to cell overproliferation in the QC, LRC
135 and endodermis, recapitulating the reported phenotype[6,7,22] (Fig. 2d).

136 When inducing Cas9p-tagRFP, we found that *ip35S* was not expressed ubiquitously but instead
137 preferentially in the root cap and sometimes in the epidermis or stele (Fig. 2a and Supplementary
138 Fig. 3). This pattern matches the domain of reduced RBR-YFP (Extended Data Fig. 5a, 5b) and
139 PLT2-3xYFP expression (Fig. 1e and Supplementary Fig. 3) after a 1-day induction of non-tagged
140 Cas9p. After long-term induction of *ip35S* or *ipWER*, PLT2-3xYFP expression decreased outside
141 the promoter-active region, in contrast to the effect on RBR (Fig. 1e, Fig. 2b, 2d and Extended Data
142 Fig. 5c). These results suggest that loss of *PLT2* in the epidermis and LRC leads to endogenous,
143 non-cell-autonomous, negative feedback regulation of *PLT2* expression in the rest of the RM,
144 leading to differentiation. In addition, our results confirm the reported cell-autonomous function of
145 RBR[6].

146 To further demonstrate the wide applicability of the IGE system, we selected *GNOM* (*GN*) as a
147 target. *GNOM* encodes a brefeldin A (BFA) sensitive ARF guanine-nucleotide exchange factor
148 (ARF-GEF) that plays essential roles in endosomal structural integrity and trafficking[23]. GNOM has

been implicated in polar localization of auxin efflux carrier (PINs), but previous studies relied on high-concentration BFA treatments or on hypomorphic alleles[24,25] because the null allele displays severe overall defects[26,27]. To test the response of PIN1 to the loss of GNOM, we made a construct using the *ipWOL* promoter to target *GNOM* in the vasculature and transformed it into both *GN-GFP*[23] and *PIN1-GFP*[28] backgrounds. Following GN-GFP signal disappearance, most transformants displayed short roots, agravitropic growth and reduced lateral root formation 10 days after germination on induction plates (Extended Data Fig. 6, 7), a similar phenotype to the *gnom* mutant[26]. We then focused on PIN1 localization. Following 3 days of induction, PIN1 lost basal polarity and its expression was strongly inhibited (Extended Data Fig. 7), confirming the role of GNOM in driving basal localization of PIN1[24,25].

When inducing editing of *PLT2*, *RBR* or *GNOM* with *ip35S* or *ipWOL*, we observed cell death in the proximal stem cells of the RM, which have been shown to be sensitive to genotoxic stress[29] (Extended Data Fig. 8). Although it has been reported that *RBR* silencing causes DNA damage and cell death[30], *PLT2* and *GNOM* have not been shown to regulate cell death before. It is thus likely that Cas9p-induced DSBs activate downstream DNA damage signals which trigger a cell death response in proximal stem cells.

Next, we tested whether a single YFP-targeting IGE construct can be used to edit several different YFP-containing complementing lines. When targeting fused *YFP* in *gPLT2-3xYFP*; *plt1,2* and *RBR-YFP*; *amiGORBR* backgrounds, we found a strong reduction in YFP followed by characteristic developmental defects (Extended Data Fig. 9), similar to targeting *PLT2* and *RBR* directly (Fig. 2b, 2d). For example, in *gPLT2-3xYFP*; *plt1,2*, editing *YFP* in the QC caused QC differentiation, though at a lower frequency than when *PLT2* was targeted (Fig. 2b and Extended Data Fig. 9b). Likewise, we observed LRC overproliferation when targeting *YFP* in *RBR-YFP*; *amiGORBR*. However, unlike when *RBR* was targeted, the YFP signal also decreased in the rest of the RM by an unknown mechanism (Fig. 2d and Extended Data Fig. 9c). Many fluorescent-tagged lines

174 complementing important genes are available, so targeting reporter-encoding genes might represent
175 a broadly applicable approach for gene function studies. Furthermore, targeting exogenous reporter
176 genes may have fewer off-target effects.

177 To compare the IGE system with artificial microRNAs (amiRNA) (Fig. 1b), a popular gene
178 knockdown strategy[31,32], we generated two amiRNAs targeting *PLT2* in *gPLT2-3xYFP*; *plt1,2*.
179 Induction of *amiPLT2-1* by *ip35S* or *ipWOX5* led to a reduction of YFP in a broader domain than
180 with IGE-PLT2 (Extended Data Fig. 10a), indicating that IGE is more specific. This is likely due to
181 cell-to-cell movement of amiRNA, consistent with the findings that several microRNAs can move[4].
182 Additionally, the IGE-caused phenotype tended to be stronger. After a 3-day induction of
183 *ip35S:amiPLT2-1*, the YFP signal was decreased but still visible, and the RM remained
184 undifferentiated after 10 days of induction (Extended Data Fig. 10a and Supplementary Table 1).
185 Likewise, no QC differentiation was observed in *ipWOX5:amiPLT2-1* lines (Extended Data Fig.
186 10a). The RM of *amiGORBR* showed an overproliferation phenotype, but it was not as severe as in
187 IGE-RBR lines (Extended Data Fig. 10b). To investigate the effect of RBR downregulation in other
188 tissues, we analyzed root secondary tissue and cotyledon epidermis. While *amiGORBR* failed to
189 show any defects in these tissues, RBR-IGE caused excessive cell divisions in pavement cells and
190 guard cells of cotyledon epidermis (as reported before[33]), as well as in periderm and phloem of root
191 secondary tissues (Extended Data Fig. 10b). This highlights a conserved role for RBR in limiting
192 cell divisions in different tissues. Interestingly, the proliferating clones were interspaced with slowly
193 proliferating WT clones, which further confirms the cell-autonomous function of RBR.

194 In conclusion, we show that the IGE system can be used to disrupt target genes efficiently and
195 precisely. Through spatiotemporal control of Cas9p expression, the system is well-suited to trace
196 early molecular and cellular changes before visible phenotypes appear. Since the estrogen inducible
197 system has been applied in various organs and plant species[14,34,35], we expect the IGE system to be

broadly applicable for plant molecular biology. By using different Cas9 variants, the system can be readily repurposed for base editing or transcriptional regulation.

METHODS

Cloning of IGE constructs

The sgRNA expression cassettes were obtained as previously described[12]. Briefly, the first round of PCR amplified *AtU3/6* promoters from template vectors, *pYLsgRNA-AtU3b* (Addgene ID: 66198), *pYLsgRNA-AtU3d* (Addgene ID: 66200), *pYLsgRNA-AtU6-1* (Addgene ID: 66202) or *pYLsgRNA-AtU6-29* (Addgene ID: 66203), using a common forward primer, *U-F*, and reverse chimeric primer *U3/6 T#-* which contains an *AtU3/6*-specific sequence at the 3' end and a target sequence at the 5' end. All sgRNA scaffolds were amplified from *pYLsgRNA-AtU3b* with a common reverse primer, *gR-R*, and chimeric forward primer *gRT #+*, which includes the sgRNA specific sequence at the 3' end and the target sequence at the 5' end. Primers used in this study are listed in Supplementary Table 2. In the second round of PCR, purified first-round PCR products were used as templates for overlapping PCR with Bsa I-containing primers *Pps/Pgs* as primer pairs. In this study, four sgRNAs (sgRNA1-sgRNA4) transcribed under promoters *AtU3b*, *AtU3d*, *AtU6-1*, and *AtU6-29*, respectively, were used to target genes of interest. For each target gene, four relatively equally distributed target sites were manually selected by following rules described previously[12]. Different sgRNA expression cassettes were cloned into the *p2R3z-Bsa I-ccdB-Bsa I* entry vector by one-step Golden Gate cloning. Golden gate cloning was performed with 120ng *p2R3z-Bsa I-ccdB-Bsa I*, 90 ng purified PCR product of each sgRNA expression cassette, 1.5µl 10x fast digestion buffer of Bsa I, 1.5µl Bsa I enzyme (15U), 1.5µl 10mM ATP, 4µl T4 DNA ligase (20U), and H_2O to make up 15µl. Before *E. coli* transformation, the reaction mixture was incubated on the thermocycler using the following conditions: 37 °C for 5 min, 16 °C for 5 min, for 30-50 cycles, then 50 °C for 5 min and 80 °C for 5 min. Alternatively, the assembly reaction can be done by incubating the reaction mixture at 37 °C for 4-6h.

The five inducible promoters (*p1R4-p35S:XVE*, *p1R4-pSCR:XVE*, *p1R4-pWER:XVE*, *p1R4-pWOL:XVE*) were created earlier[13]. To construct the binary vector, a MultiSite Gateway LR reaction was performed with the inducible promoters in the 1st box, *Cas9p*, *dCas9p*, *Cas9p-tagRFP* or *amiPLT2* in the 2nd box, the sgRNA expression cassette or *nosT* terminator in the 3rd box and *pBm43GW* (PPT (phosphinotricin) selection) or *pFRm43GW* (seed coat RFP selection) as the destination vectors. The detailed cloning procedures of vectors *p221z-Cas9p-t35s* (Addgene ID: 118385), *p221z-Cas9p-tagRFP-t35s* (Addgene ID: 118386), *p221z-dCas9p-t35s* (Addgene ID: 118387), *p2R3z-Bsa I-ccdB-Bsa I* (Addgene ID: 118389), *p221z-AtMIR390a* (Addgene ID: 118388), *p2R3z-AtU3b-tRNA-ccdB-sgRNA* (Addgene ID: 118390) and non-destructive fluorescent screening vectors *pFRm43GW* (Addgene ID: 133748) and *pFG7m34GW* (Addgene ID: 133747) are described in the Supplementary Methods. All constructs generated in this study are listed in Supplementary Table 3.

Transformation of the IGE constructs into *Arabidopsis*

PLT2-targeting constructs were transformed into the *gPLT2-3xYFP*; *plt1,2* background[18]. For *RBR*-targeting constructs, the transformed background was segregating *pRBR:RBR-YFP*(+,-); *35S:amiGORBR*(+,+)[22]. The IGE construct targeting *GNOM* was transformed into both the *GN-GFP*[23] and *PIN1-GFP*[28] backgrounds. With the exception of the construct transformed into the GN-GFP background, in which the GFP signal was weak, all T1 lines were prescreened under a fluorescence-binocular microscope to identify those with leaky inducible promoter or in which the root tip had been damaged during selection. Only lines with YFP/GFP signal in root tip were used for further experiments. The above-mentioned *PLT2* and *RBR*-based backgrounds were also used in transformation of the *YFP*-targeting construct. The *RBR*-targeting construct *ip35S>>Cas9p-RBR* was also transformed into the *Col-0* background. All experiments were conducted using T1 plants unless stated otherwise.

Plant growth and chemical treatments

All seeds were surface-sterilized with 20% chlorine for 1 min, followed by a 1 min incubation in 70% ethanol and two rinses in H_2O. The sterilized seeds were kept at 4°C for two days before plating on half strength Murashige and Skoog growth medium (½ GM) plates with/without selection antibiotics. The plates were vertically positioned in a growth chamber at 22 °C in long day conditions. PPT selection was conducted by growing sterilized seeds on ½ GM plates containing 20 μg/ml PPT for 4 days, then transferring them to PPT-free ½ GM plates for another 2 days before treatment. The transgenic seeds containing pFRm43GW were screened under a fluorescence binocular using DSRed filter (Extended Data Fig. 1b), and the sterilized seeds were directly grown on ½ GM plates for 6 days before treatment. 17-β-estradiol (17-β, Sigma) was dissolved in dimethyl sulfoxide (DMSO, Sigma) to make 10 mM stock solution (stored at -20°C) and a 5 μM working concentration was used. Mock or 17-β treatment was performed by transferring seedlings on ½ GM plates containing equal volume of DMSO or 17-β. Alternatively, screened seeds were germinated on DMSO or 17-β containing ½ GM plates.

Microtome sectioning and histological staining

Transverse plastic sections were cut from *ip35S>>Cas9p-RBR* (in *Col-0* background) roots which were geminated on estradiol plates for 20 days, as well as *Col-0* and *35S:amiGORBR* roots that were grown on ½ GM plates for 20 days. Sections from 5 mm below the root–hypocotyl junction point were used for analysis. Sections were stained in 0.05% (w/v) ruthenium red solution (Fluka Biochemika) for 5 seconds before microscopy analysis. For root samples from *ipWOX5>>Cas9p-tagRFP-PLT2*, *ipWOX5>>Cas9p-tagRFP-YFP* and *ipWOX5>>amiPLT2-1*, after 3 days of mock or 17-β treatment, a serial longitudinal section of 5 μm thickness was cut from the root tips. To observe the QC differentiation state, the longitudinal sections were stained in 1g/ml lugol solution (Sigma) for 12 seconds before observation under a microscope. The sectioning methodology has been previously described[36].

Microscopy and image processing

All of the cross sections and longitudinal sections were visualized using a Leica 2500 microscope. All fluorescent images were taken with a Leica TCS SP5 II Confocal microscope. Root samples used for cell death detection were stained in 10 μg/mL propidium iodide for 10 min then rinsed twice in water before imaging. For other samples used for fluorescence observation, a ClearSee protocol[37] was used with slight modifications. Samples were first fixed in 4% paraformaldehyde (dissolved in 1xPBS, PH 7.2) for at least one hour with vacuuming, then washed twice in 1x PBS and transferred to ClearSee solution. Samples were incubated in ClearSee solution for at least 24h. Before imaging, 0.1% calcofluor white dissolved in ClearSee was used for one hour with vacuuming to stain cell walls. This was followed by washing the samples in ClearSee solution for at least 30 min with shaking. During the washing, the ClearSee solution was changed every 15 min. Confocal settings were kept the same between mock and induction in each experiment. All confocal images were acquired in sequential scanning mode. Images were sometimes rotated using Photoshop and the resulting empty corners were filled with a black background. All images were cropped and organized in Microsoft PowerPoint. The brightness of the calcofluor signal was sometimes adjusted differently between the mock and induction for better cell wall visualization.

Protoplasting and FACS

T2 lines of *ipWER>>Cas9p-tagRFP-PLT2* in *gPLT2-3xYFP*; *plt1,2* (#1, #2, #5 and #8); *ipWOL>>Cas9p-tagRFP-PLT2* in *gPLT2-3xYFP*; *plt1,2* (#1 and #2) with four sgRNAs; T1 lines of *ipWER>>Cas9p-tagRFP-PLT2-sgRNA1* in *gPLT2-3xYFP*; *plt1,2* and *ipWOL>>Cas9p-tagRFP-PLT2-sgRNA1* in *gPLT2-3xYFP*; *plt1,2* with only sgRNA1 were used for protoplast preparation. T2 seeds were planted on top of nylon mesh (100 μm, NITEX), which was placed on surface of ½ GM without adding PPT. After 6 days of germination, the induction was conducted by transferring mesh together with the seedlings to 17-β plates. For T1 lines, transgenic positive seedlings were first screened on PPT plates for 4 days, then transferred to ½ GM plates for another two days before 17-

297 β induction. An equal amount of *Ws* (Wassilewskija ecotype) and *gPLT2-3xYFP*; *plt1,2* seeds were
298 also planted at the same time to facilitate gate determination in sorting.

299 The protoplast preparation was done as previously described[38]. The protoplasting solution (pH 5.7)
300 consists of 1.25% (w/v) cellulase-R10 (Yakult), 0.3% (w/v) macerozyme-R10 (Yakult), 0.4 M
301 mannitol, 20 mM MES, 20 mM KCl, 0.1% (w/v) BSA, and 10 mM $CaCl_2$. For each sample, more
302 than 600 root tips were harvested and incubated in 10 mL protoplasting solution at room
303 temperature for 90 min. A shaker (75 rpm) was used to facilitate protoplast disassociation. The
304 resultant protoplast solution was filtered through a 70μm filter. The flow-through was transferred
305 into a 15mL falcon tube and centrifuged at 400g for 6 min. The precipitated protoplasts were
306 resuspended with protoplasting solution without cellulase and macerozyme before conducting a
307 three-laser (blue 488 nm, red 633 nm, Near UV 375 nm) BD FACS AriaII cell sorting analysis.
308 Widely apart fluorescence detectors (PE-Texas Red 616/23 for RFP and FITC 530/30 for YFP) were
309 used to reduce fluorescence spillover effect and gates were determined against controls (Ws and
310 *gPLT2-3xYFP; plt1,2*) to minimize the false positive events within respective population. Because
311 of high background autofluorescence and the clear separation of the fluorescent-positive
312 populations, the Cas9p-tagRFP positive and PLT2-3xYFP positive populations were sorted without
313 fluorescence compensation.

314 **Quantitative PCR**

315 We isolated DNA from sorted protoplasts based on previously described method[39]. Using genomic
316 DNA as template, qPCR was performed on a Bio-Rad CFX384 cycler with EvaGreen qPCR mix
317 (Solis Biodyne), by following the manufacturer's instructions. Pooled DNA isolated from *gPLT2-*
318 *3xYFP*; *plt1,2* background was used as control. To avoid the interference of native *PLT2*, the
319 forward primer was designed on LR reaction residual region, attB1, a linker between the promoter
320 *PLT2* and genomic *PLT2*. For each DNA sample, qPCR was performed three times with three

technical repeats for each. The relative none-truncated DNA level of *PLT2-3xYFP* in each sample was normalized to the reference gene *UBQ10*[40]. The primers are listed in Supplementary Table 2.

PCR for TIDE analysis

TIDE analysis uses Sanger sequencing data as an input to predict genome editing efficiency in DNA samples[20]. For DNA samples containing four sgRNAs, two PCR amplification steps were conducted to obtain corresponding fragment harboring each target site. In the 1st PCR step, transgenic *PLT2* genomic fragment was amplified (26 cycles) by using a primer pair spanning four sgRNAs target sites. Then WT size band was gel purified and used as template in the 2nd PCR step. In the 2nd PCR, the DNA fragment around each sgRNA target site was amplified with 30 PCR cycles. Corresponding fragments were amplified from plasmid *pPLT2-gPLT2-3xYFP*[18] as control. The PCR product was purified from gel for Sanger sequencing. The mutation efficiency at each target site was estimated by TIDE analysis (https://tide.deskgen.com/). For DNA samples in which *PLT2* was targeted only by sgRNA1, the region including the target site was amplified in two PCR amplification steps, as explained above. PCR products after 1st PCR step were compared to the product after the 2nd step: both TIDE analysis and amplicon sequencing showed similar estimated editing efficiencies between the two products (Supplementary Data 2). This indicates that the second amplification step did not distort the results (i.e. estimated editing efficiencies). The primers used for PCR amplification and Sanger sequencing are listed in Supplementary Table 2.

Amplicon sequencing

To confirm the TIDE analysis results, we selected four pooled DNA samples from sorted T1 lines of *ipWER>>Cas9p-tagRFP-PLT2-sgRNA1* and *ipWOL>>Cas9p-tagRFP-PLT2-sgRNA1* for amplicon sequencing (Supplementary Data 2). We first amplified (26 cycles) a 316bp-long fragment around the target site with the forward primer located at the attB1 region of the transgenic construct. Even we performed PCR with 6x 50µL reaction volumes for each sample, the resulting yield was

relatively low, from which we did nested PCR (30 cycles) and obtained a 266bp-long fragment with high yields. These 2nd round PCR products for each sample were used for amplicon sequencing. To evaluate the effect of our PCR amplification strategy on mutation efficiency estimation, we also selected two low yield 1st round PCR products for amplicon sequencing (Supplementary Data 2).

DNA libraries of these six PCR products were constructed, and 150-bp paired-end reads were generated using an Illumina NovaSeq PE150 platform (Novogene, Tianjin, China). Between 6.87e6 and 9.47e6 reads were obtained for each of the six samples. First 100,000 reads from each sample were aligned with bwa mem[41] (v.0.7.15) to either 316 bp-long (26 PCR cycles) or 266 bp-long (30 PCR cycles) reference sequence using program's default settings. More than 99.77% of the reads mapped, giving ~93,000X and ~112,000X coverage for the longer and the shorter reference sequence, respectively. Read were realigned around indels using GATK3 IndelRealigner[42] (v.3.7.0) and program's default settings. Variants were called with GATK4 Mutect2[43] (v.4.1.4) using the single-sample mode and unsetting the maximum number of reads (max-reads-per-alignment-start 0). The variant calls were reformatted and allelic depths printed with BCFtools query[44] (v.1.9-87).

DATA AND MATERIALS AVAILABILITY

Vectors created in this study have been deposited in Addgene for distribution. Addgene ID numbers are presented in Fig. 1, and Extended Data Fig. 1. All plant material, expression constructs and data supporting findings of this study are available from the corresponding author upon request.

ACKNOWLEDGEMENT

We thank B. Scheres (Wageningen University) and N. Geldner (University of Lausanne) for sharing published materials; N. Geldner for providing support for R.U.; K. D. Birnbaum (Univeristy of New York) for helpful discussion; T. Pessa-Morikawa (University of Helsinki) for technical support on FACS; A. Vaten (University of Helsinki) for cotyledon epidermis imaging and S. el-Showk for proofreading of this manuscript. This work was supported by the Academy of Finland (grants

#316544, #266431, #307335), European Research Council (ERC-CoG CORKtheCAMBIA, agreement 819422), University of Helsinki HiLIFE fellowship (X.W., L.Y., M.L., A.P.M.) and European Molecular Biology Organisation (EMBO ALTF 1046-2015 to R.U.). X.W. is also supported by a grant from the Chinese Scholarship Council (CSC).

CONTRIBUTIONS

X.W. and A.P.M. designed the experiments. X.W. conducted all experiments, except L.Y. carried out the analysis for Supplementary Table 1, and M.L. performed FACS. R.U. generated and tested the new destination vectors. A.L. determined the indel mutation efficiency of amplicon deep sequencing. X.W. and A.P.M. analyzed the results and wrote the manuscript, with input from all co-authors.

COMPETING INTERESTS STATEMENT

The authors declare no competing financial interests.

FIGURE LEGENDS

Figure 1: Engineering the IGE system for conditional genome editing.

a, Cloning steps for IGE construct generation. The sgRNA expression cassette (*pAtU3/6-sgRNA*) was constructed in two PCR steps followed by Golden Gate cloning into the *p2R3z-Bsa I-ccdB-Bsa I* entry vector. The final IGE construct was then recombined by a MultiSite Gateway LR reaction. **b**, Schematics of two other entry vectors generated in this study. Entry vector *p221z-AtMIR390a*, in which *AtMIR390a* is split by a *Bsa I*- flanking-*ccdB* cassette, was utilized for inducible gene knockdown. Entry vector *p2R3z-AtU3b-tRNA-ccdB-gRNA* was generated to exploit the endogenous tRNA processing system. Two annealing and overlapping target sequences with overhangs can be directly ligated into Bsa I-linearized *p2R3z-AtU3b-tRNA-ccdB-gRNA*. Red numbers in brackets are the Addgene numbers of vectors created in this study. **c**, The YFP signal in the RM of 7 day-old

392 *gPLT2-3xYFP*; *plt1,2*. **d**, dCas9p does not decrease PLT2-3xYFP expression. **e**, Cas9p induction
393 resulted in a gradual loss of YFP and eventually full differentiation of the RM. The numbers are the
394 frequency of the observed phenotypes in independent T1 samples. Cell walls are visualized by
395 calcofluor. Experiments were repeated three times in **c**-**e**. Scale bar, 50 μm.

396 **Figure 2: The IGE system enables efficient cell-type-specific genome editing**

397 **a**, A one-day induction is sufficient to remove PLT2-3xYFP expression in a cell-type specific
398 manner. In rare occasions, we observed overlapping Cas9p-tagRFP and PLT2-3xYFP expression
399 (white arrowhead). **b**, PLT2 is cell-autonomously required for QC and stem cell maintenance. QC
400 cells (red arrowheads) as well as endodermal and epidermal cells (white arrows) showed premature
401 differentiation or cell expansion after 3 days of induction. QC differentiation is accompanied by
402 shift of *ipWOX5* expression towards the provascular cells. Removal of PLT2 from the *ipWER*
403 expression domain resulted in fewer LRC layers (white arrowhead) and ectopically decreased
404 PLT2-3xYFP expression. Cas9p-tagRFP expression in the LRC and epidermis was frequently
405 undetectable. **c**, A one-day induction is sufficient to induce efficient cell-type specific RBR editing.
406 Without induction, the QC frequently shows cell divisions, probably due to the heterogeneity of the
407 complementing RBR-YFP. **d**, RBR cell-autonomously prevents QC and stem cell division. The
408 endodermis, QC and LRC exhibited overproliferation after 3 days of induction. White arrowheads
409 indicate rotated cell division planes in the endodermis. Brackets in c and d indicate QC regions. Cell
410 walls are highlighted by calcofluor. The numbers represent the frequency of the observed
411 phenotypes in independent T1 samples. All experiments were repeated at least three times. Scale
412 bars, 50 μm.

413 **REFERENCES**

414 1. Candela, H., Perez-Perez, J. M. & Micol, J. L. *Trends Plant Sci.* **16**, 336-345 (2011).
415 2. Borghi, L. *et al. Plant Cell* **22**, 1792-1811 (2010).
416 3. Guo, J., Wei, J., Xu, J. & Sun, M. X. *J. Exp. Bot.* **65**, 1165-1179 (2014).

417 4. Liu, L. & Chen, X. *Nat. Plants* **4**, 869-878 (2018).
418 5. Heidstra, R., Welch, D. & Scheres, B. *Genes Dev.* **18**, 1964-1969 (2004).
419 6. Wachsman, G., Heidstra, R. & Scheres, B. *Plant Cell* **23**, 2581-2591 (2011).
420 7. Wildwater, M. *et al. Cell* **123**, 1337-1349 (2005).
421 8. Qi, Y. P. *et al. G3* **3**, 1707-1715 (2013).
422 9. Christian, M., Qi, Y. P., Zhang, Y. & Voytas, D. F. *G3* **3**, 1697-1705 (2013).
423 10. Mao, Y. F., Botella, J. R., Liu, Y. G. & Zhu, J. K. *Natl. Sci. Rev.* **6**, 421-437 (2019).
424 11. Decaestecker, W. *et al. Plant Cell* **31**, 2868-2887 (2019).
425 12. Ma, X. *et al. Mol. Plant* **8**, 1274-1284 (2015).
426 13. Siligato, R. *et al. Plant Physiol.* **170**, 627-641 (2016).
427 14. Zuo, J., Niu, Q. W. & Chua, N. H. *Plant J.* **24**, 265-273 (2000).
428 15. Karimi, M., Inze, D. & Depicker, A. *Trends Plant Sci.* **7**, 193-195 (2002).
429 16. Aida, M. *et al. Cell* **119**, 109-120 (2004).
430 17. Galinha, C. *et al. Nature* **449**, 1053-1057 (2007).
431 18. Mähönen, A. P. *et al. Nature* **515**, 125-129 (2014).
432 19. Vandenberg, C., Willemsen, V., Hage, W., Weisbeek, P. & Scheres, B. *Nature* **378**, 62-65 (1995).
433 20. Brinkman, E. K., Chen, T., Amendola, M. & van Steensel, B. *Nucleic Acids Res.* **42**, e168
434 (2014).
435 21. Ebel, C., Mariconti, L. & Gruissem, W. *Nature* **429**, 776-780 (2004).
436 22. Cruz-Ramirez, A. *et al. PLoS Biol.* **11** (2013).
437 23. Geldner, N. *et al. Cell* **112**, 219-230 (2003).
438 24. Kleine-Vehn, J. *et al. Curr. Biol.* **18**, 526-531 (2008).
439 25. Steinmann, T. *et al. Science* **286**, 316-318 (1999).
440 26. Geldner, N. *et al. Development* **131**, 389-400 (2004).
441 27. Shevell, D. E. *et al. Cell* **77**, 1051-1062 (1994).

442 28. Scarpella, E., Marcos, D., Friml, J. & Berleth, T. *Genes Dev.* **20**, 1015-1027 (2006).
443 29. Fulcher, N. & Sablowski, R. *Proc. Natl. Acad. Sci. USA* **106**, 20984-20988 (2009).
444 30. Horvath, B. M. *et al. Embo J.* **36**, 1261-1278 (2017).
445 31. Carbonell, A. *et al. Plant Physiol.* **165**, 15-29 (2014).
446 32. Schwab, R., Ossowski, S., Riester, M., Warthmann, N. & Weigel, D. *Plant Cell* **18**, 1121-1133
447 (2006).
448 33. Matos, J. L. *et al. Elife* **3** (2014).
449 34. Brand, L. *et al. Plant Physiol.* **141**, 1194-1204 (2006).
450 35. Moore, I., Samalova, M. & Kurup, S. *Plant J.* **45**, 651-683 (2006).
451 36. Kareem, A. *et al. Plant Methods* **12**, 27 (2016).
452 37. Ursache, R., Andersen, T. G., Marhavy, P. & Geldner, N. *Plant J.* **93**, 399-412 (2018).
453 38. Bargmann, B. O. & Birnbaum, K. D. *J. Vis. Exp.* (2010).
454 39. Edwards, K., Johnstone, C. & Thompson, C. *Nucleic Acids Res.* **19**, 1349 (1991).
455 40. Smetana, O. *et al. Nature* **565**, 485-489 (2019).
456 41. Li, H., Preprint at http://arxiv.org/abs/1303.3997 (2013).
457 42. McKenna, A. *et al. Genome Res.* **20**, 1297-1303 (2010).
458 43. Poplin, R. *et al.*, Preprint at https://www.bioRxiv.org/content/10.1101/201178v201172 (2018).
459 44. Li, H. *et al. Bioinform.* **25**, 2078-2079 (2009).

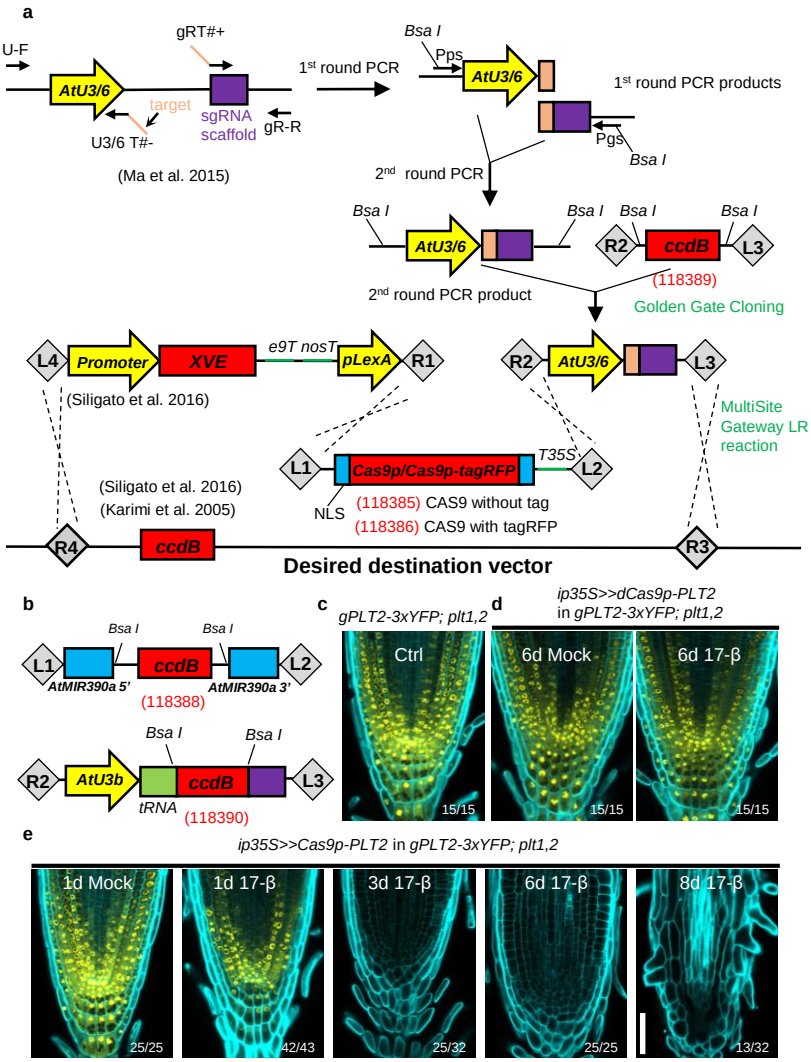

Figure 1: Engineering the IGE system for conditional genome editing.

a, Cloning steps for IGE construct generation. Fusions of the sgRNA expression cassette (*pAtU3/6-sgRNA*) were constructed by two PCR steps and were subsequently cloned into the *p2R3z-Bsa I-ccdB-Bsa I* entry vector by Golden Gate cloning. The binary IGE construct was then recombined by a MultiSite Gateway LR reaction. **b**, Schematics of two other entry vectors generated in this study. Entry vector *p221z-AtMIR390a*, in which *AtMIR390a* is split by a *Bsa I*- flanking-*ccdB* cassette, was utilized for inducible gene knockdown. Entry vector *p2R3z-AtU3b-tRNA-ccdB-gRNA* was generated to exploit the endogenous tRNA processing system. Two annealed overlapping target sequences with overhangs can be directly ligated into *Bsa I*-linearized *p2R3z-AtU3b-tRNA-ccdB-gRNA*. Red numbers in brackets are the Addgene numbers of vectors created in this study. **c**, The YFP signal in the RM of 7 day-old *gPLT2-3xYFP*; *plt1,2*. **d**, dCas9p does not decrease PLT2-3xYFP expression. **e**, Cas9p induction resulted in a gradual loss of YFP and eventually full differentiation of the RM. The numbers are the frequency of the observed phenotypes in independent T1 samples. Cell walls are visualized by calcofluor. Experiments were repeated three times in **c**-**e**. Scale bar, 50 μm.

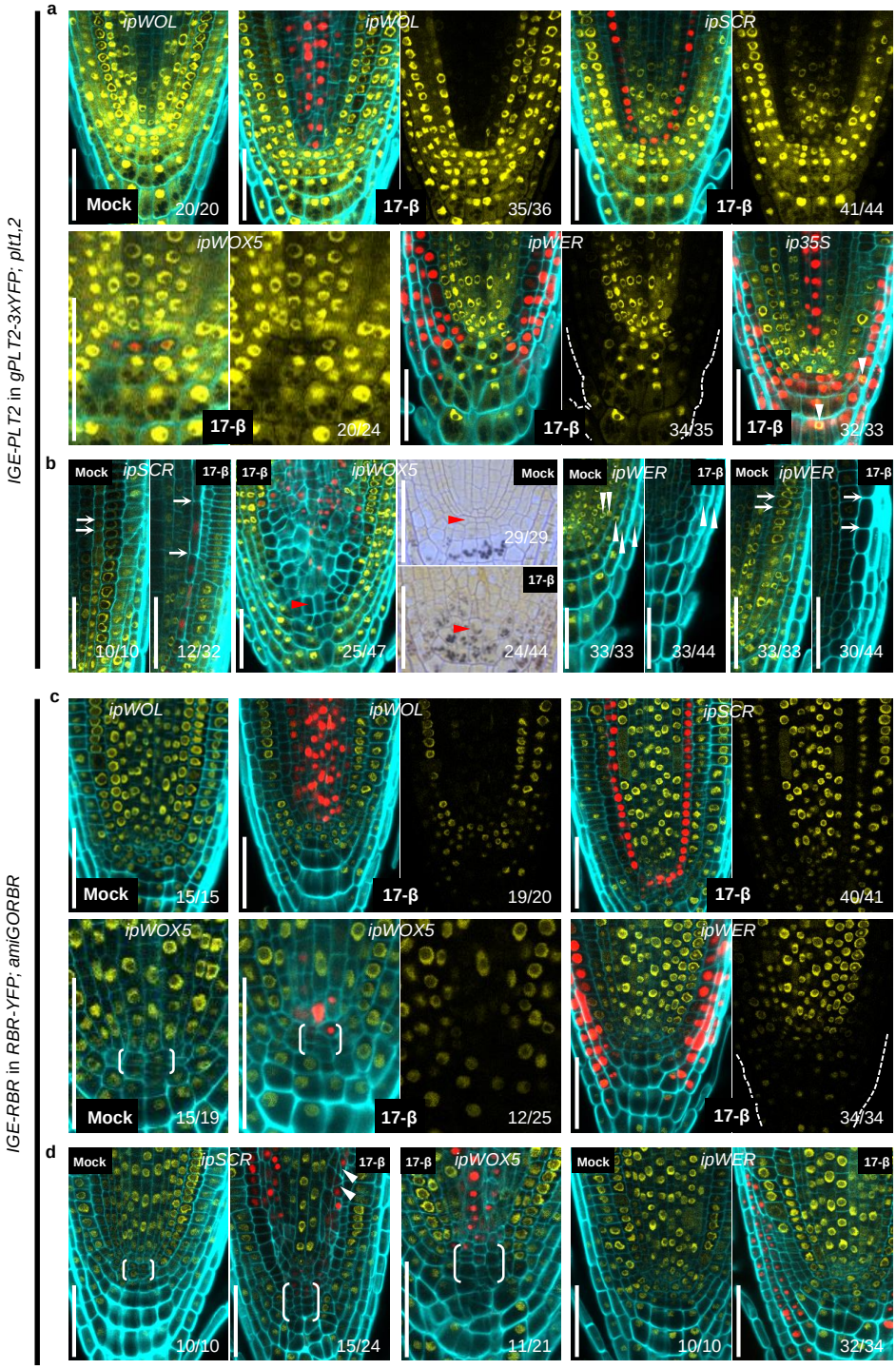

Figure 2: The IGE system enables efficient cell-type-specific genome editing

a, A one-day induction is sufficient to remove PLT2-3xYFP expression in a cell-type specific manner. In rare occasions, we observed overlapping Cas9p-tagRFP and PLT2-3xYFP expression (white arrowhead). **b**, PLT2 is cell-autonomously required for QC and stem cell maintenance. QC cells (red arrowheads) as well as endodermal and epidermal cells (white arrows) showed premature differentiation or cell expansion after 3 days of induction. QC differentiation is accompanied by shift of *ipWOX5* expression towards the provascular cells. Removal of PLT2 from the *ipWER* expression domain also resulted in fewer LRC layers (white arrowhead) and ectopically decreased the PLT2-3xYFP expression. Cas9p-tagRFP expression in the LRC and epidermis was frequently undetectable. **c**, A one-day induction is sufficient to induce efficient cell-type specific *RBR* editing. Without induction, the QC frequently shows cell divisions, probably due to the heterogeneity of the complementing RBR-YFP. **d**, RBR cell-autonomously prevents QC and stem cell division. The endodermis, QC and LRC exhibited overproliferation after 3 days of induction. White arrowheads indicate rotated cell division planes in the endodermis. Brackets in **c** and **d** indicate QC regions. Cell walls are highlighted by calcofluor. The numbers represent the frequency of the observed phenotypes in independent T1 samples. All experiments were repeated at least three times. Scale bars, 50 µm.

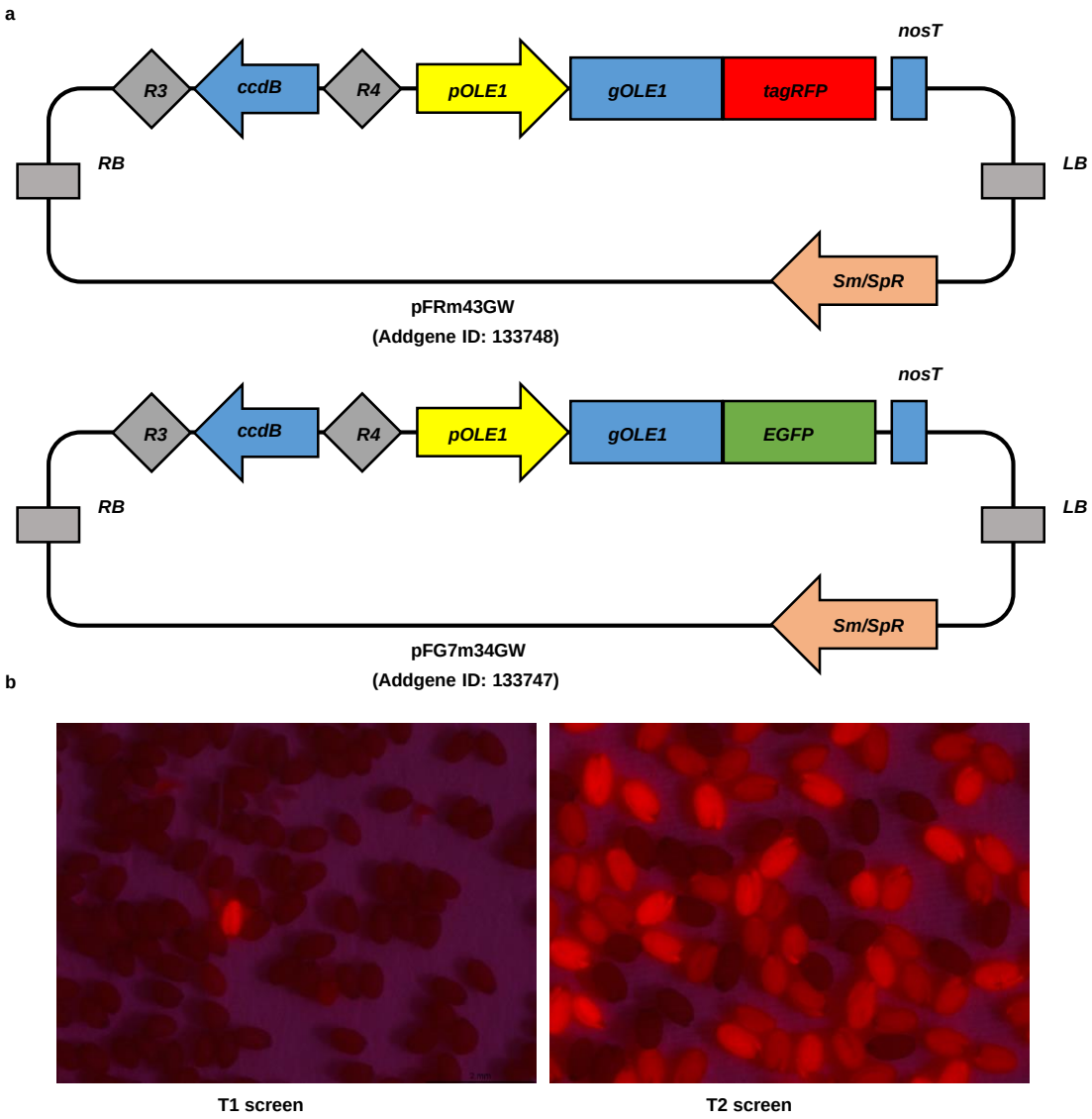

Extended Data Figure 1 Non-destructive screening markers facilitate identification of transformed seeds.

(a) Non-destructive fluorescent screening destination vectors generated in this study. **(b)** Examples of transgenic seeds containing pFRm43GW screened under the fluorescence-binocular in the T1 (left) and T2 (right) generations. Experiments in **(b)** have been repeated more than three times.

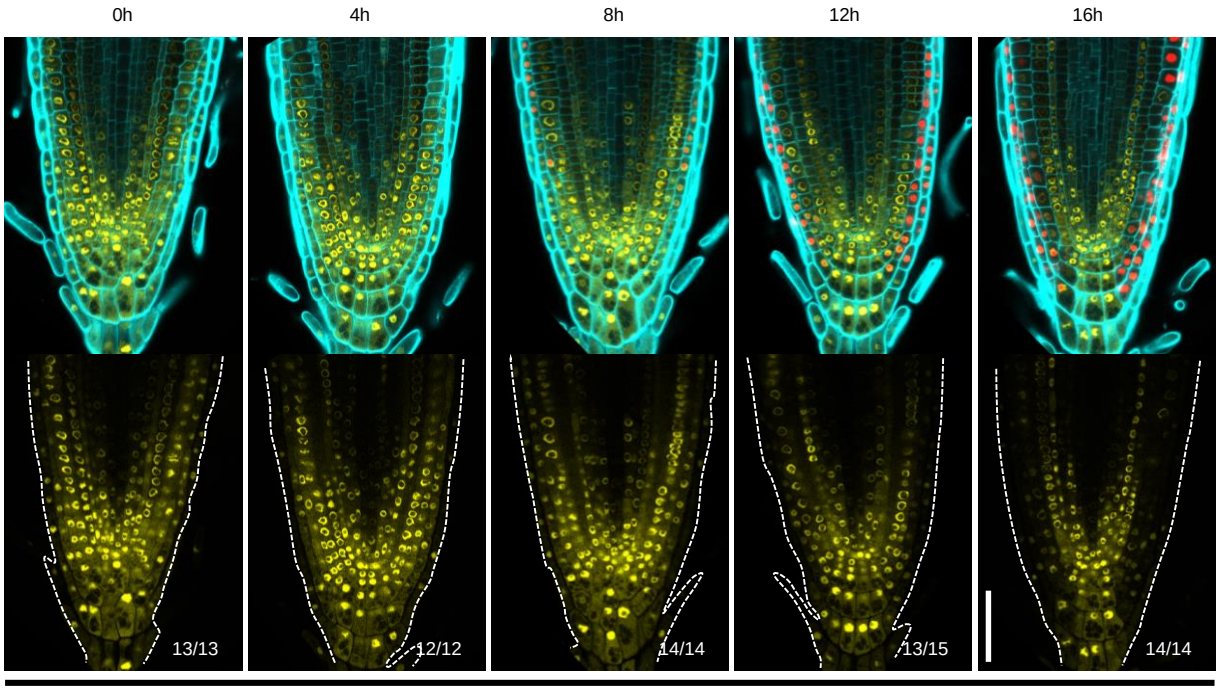

ipWER>>Cas9p-tagRFP-PLT2 in *gPLT2-3xYFP*; *plt1,2,*

Extended Data Figure 2 IGE system enables real time observation of genome editing.

To monitor *PLT2* editing dynamics, a time-course 17-β induction was conducted to *ipWER>>Cas9p-tagRFP-PLT2* in *gPLT2-3xYFP*; *plt1,2* (T2 generation, line #1). Cas9p-tagRFP fluorescence appeared after 4 hours of induction, followed by gradual reduction of PLT2-3xYFP expression (starting after 12 hours of induction). Cas9p-tagRFP expression and editing activity was gradually spread inwards, likely due to the radial diffusion of 17-β within *ipWER* domain. White dotted lines mark the RM outlines. Cell walls are visualized by calcofluor. Experiments were repeated three times. Numbers indicate the frequency of observed phenotype within given induction duration. Scale bar, 50 μm.

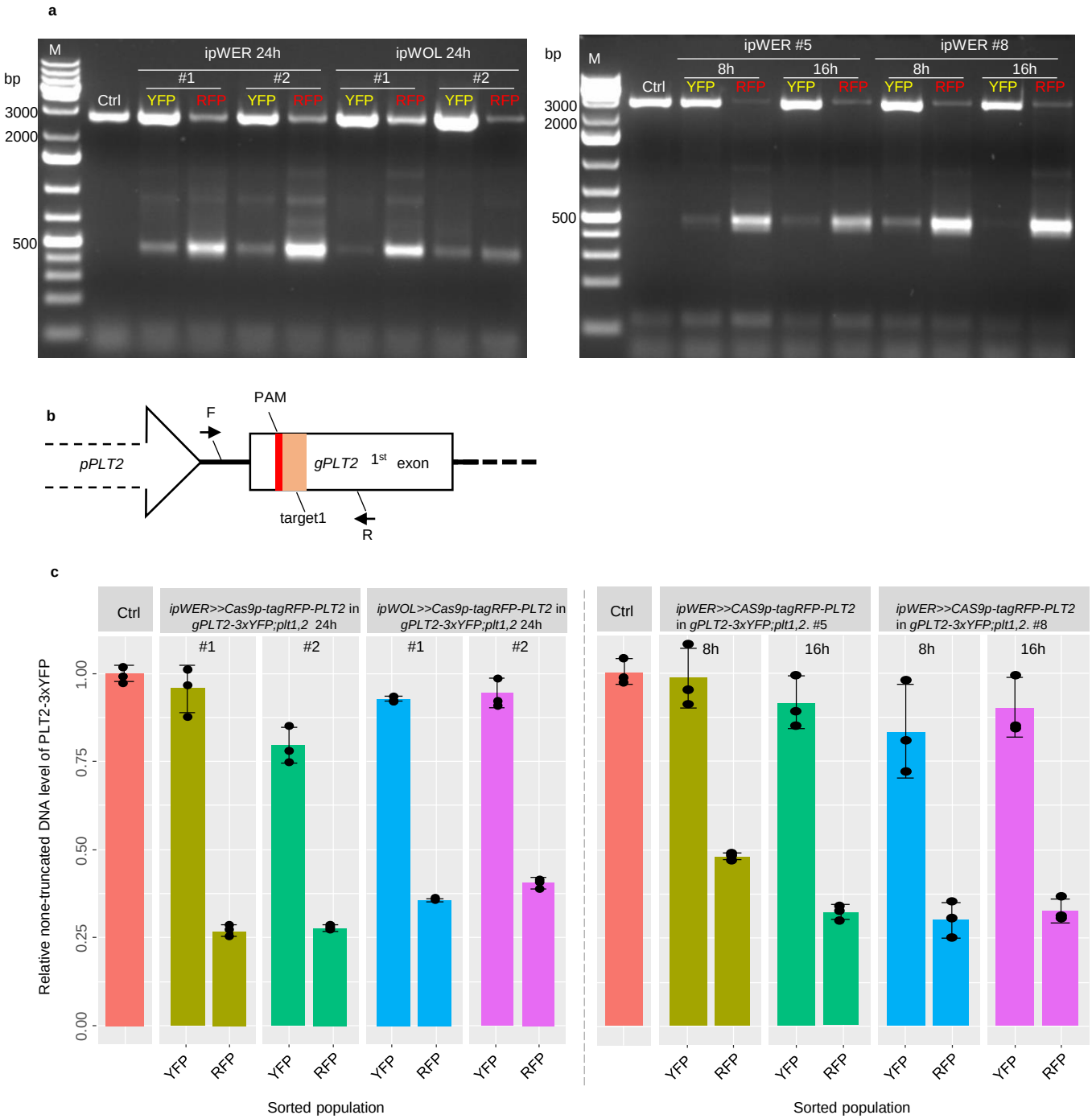

Extended Data Figure 3 Detection and quantification of *PLT2* deletion from sorted cell populations

(**a**) PCR-based detection of *PLT2* deletion in sorted cell populations. While several truncated bands were visible, the predominant truncated band corresponds to the large fragment deletion between target1 and target4 (see location of target sites in Supplementary Fig. 1). Experiments were repeated three times. (**b**) qPCR primer design strategy for *PLT2* deletion efficiency quantification. To avoid amplification of native *PLT2*, forward primer (F) was designed at attB1 site linking promoter and genomic *PLT2* and reverse primer (R) was designed at downstream of target1. (**c**) Quantification of *PLT2* deletion efficiency by qPCR with the pooled genome DNA from the sorted population (n>600) as template. Error bars represent s.d., and experiments were repeated three times with similar results. Individual values (black dots) and means (bars) are shown. Ctrl indicates the *gPLT2-3xYFP*; *plt1,2*.

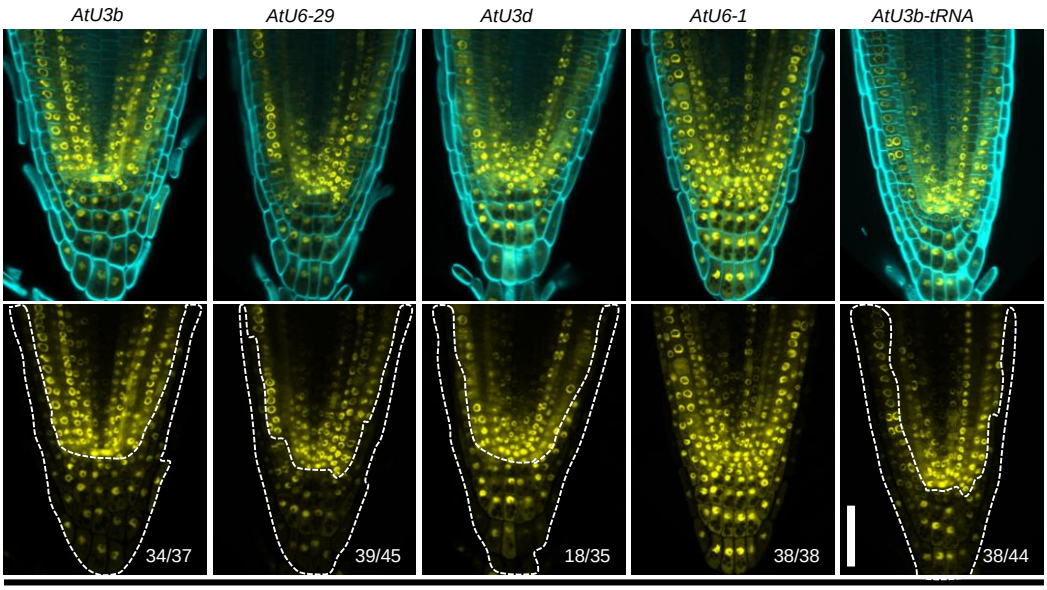

Extended Data Figure 4 sgRNA promoter identity affects editing efficiency in *Arabidopsis* roots.

For each construct, the indicated sgRNA promoter was used to drive transcription of sgRNA1, while *ip35S* was used to guide *Cas9p* transcription. *AtU3b* and *AtU6-29* showed the highest editing efficiency in T1 seedlings after one-day of induction (1d 17-β). This may explain the preferred detection of deletion between target1 (*AtU3b*) and target4 (*AtU6-29*) when four sgRNAs were used in a single construct (Supplementary Fig. 4 and Extended Data Fig. 3a). Transcription of tRNA together with sgRNA1 under the *AtU3b* promoter also resulted in efficient *PLT2* editing. White dotted lines mark the region with reduced YFP signal. This corresponds to the region where ip35S is active (Fig. 2a and Supplementary Fig. 3). Cell walls are highlighted by calcofluor. Numbers indicate the frequency of similar results in the independent T1 samples analyzed. All experiments were repeated three times. Scale bar, 50 μm.

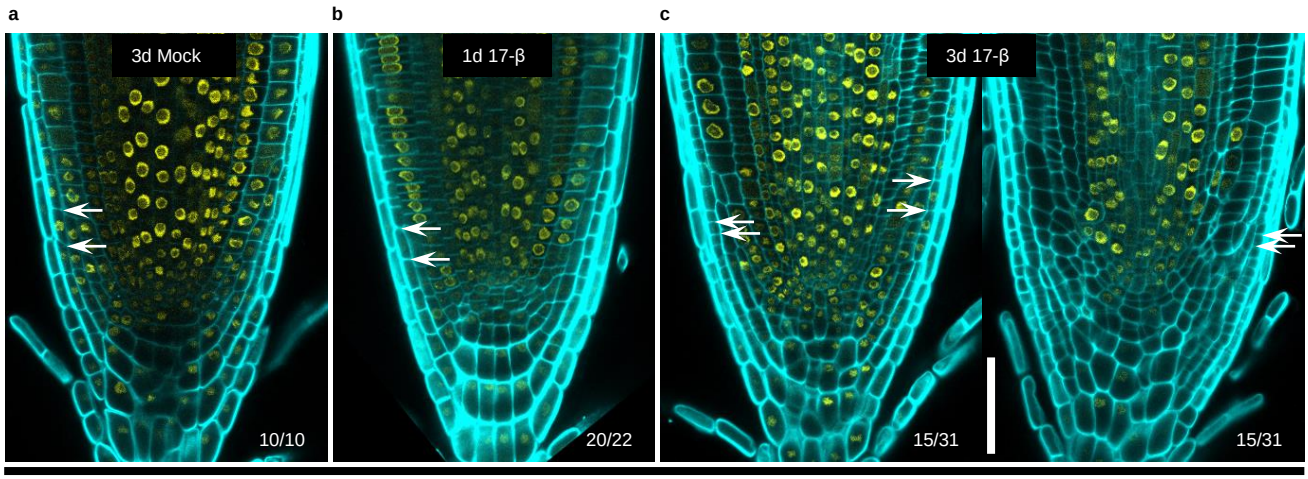

ip35S>>Cas9p-RBR in *RBR-YFP*; *amiGORBR*

Extended Data Figure 5 RBR functions cell-autonomously in the RM.

(a) A three-day mock treatment of *ip35S>>Cas9p-RBR* in *RBR-YFP; amiGORBR*. **(b)** A one-day induction caused a reduced RBR-YFP signal mainly in the root cap region without an obvious phenotype. **(c)** A three-day induction of *RBR* editing with *ip35S* typically led to LRC overproliferation (white arrows) without affecting the YFP signal in other domains. While half of the transformants showed sectors of variable size lacking RBR-YFP expression (left panel in **c**), the other half showed almost complete absence of RBR-YFP in the domain of *ip35S* (right panel). Cell walls are visualized by calcofluor. Numbers indicate the frequency of the observed phenotype in independent T1 samples. Experiments were repeated three times. Scale bar, 50 μm.

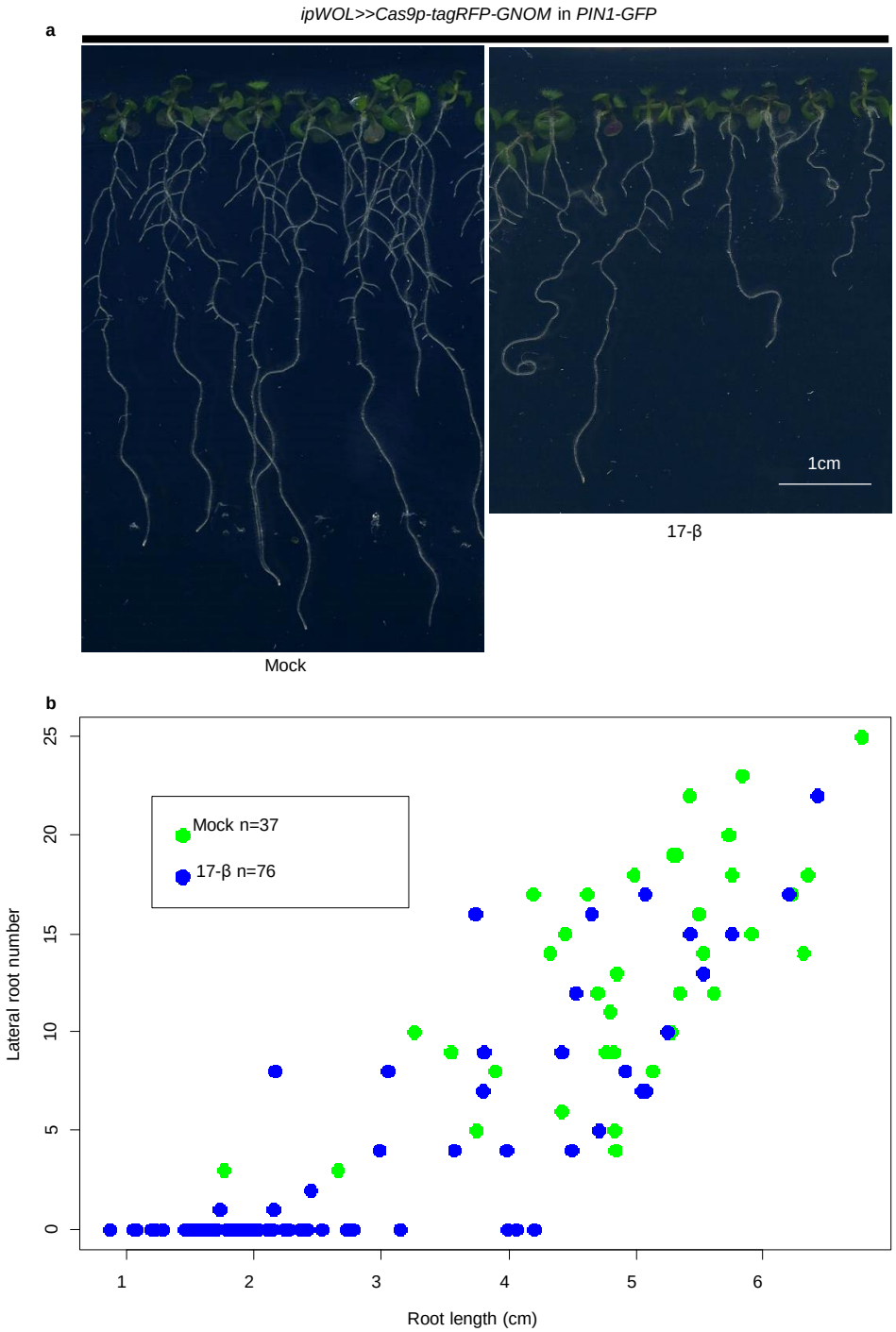

Extended Data Figure 6 Post-embryonically inducing *GNOM* editing recapitulates the phenotypes of the *gnom* mutant.

(a) Plants with *ipWOL>>Cas9p-tagRFP-GNOM* in *PIN1-GFP* after ten days germination on mock or 17-β plates. Inducing *GNOM* editing led to shorter roots, agravitropic growth and decreased lateral root (LR) numbers. Adventitious roots from the hypocotyl were frequently found, however these roots were not counted in LR quantification. For each independent root, LR number and root length is plotted in **(b)**. Experiments were repeated three times. Scale bar, 1 cm.

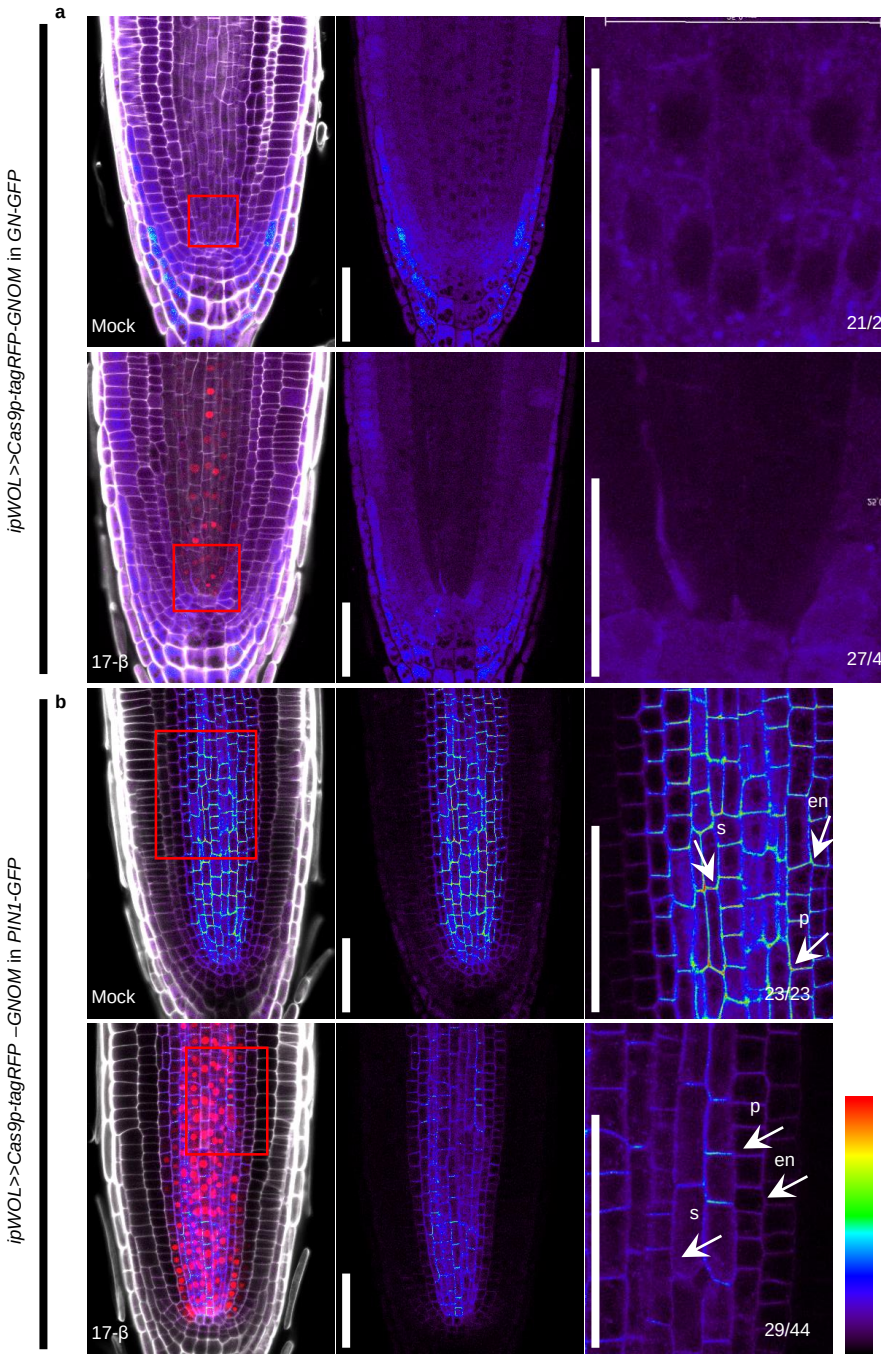

Extended Data Figure 7 GNOM is required for PIN1 polarity and expression.

(a) *GNOM* expression disappeared from the vasculature after a 6-day induction of *ipWOL>>Cas9p-tagRFP-GNOM* in *GN-GFP*. Due to the weak GFP signal, only roots showing a clear loss of GFP signal were included in quantification. **(b)** A three-day induction of *ipWOL>>Cas9p-tagRFP-GNOM* in *PIN1-GFP* resulted in loss of polarity and decreased expression of PIN1-GFP in the endodermis (en), pericycle (p) and stele (s) (white arrows). Right panels are magnified images of the regions marked with a red box in the left panels. Cell walls are marked by calcofluor. Numbers indicate the frequency of the observed phenotype in independent T1 samples analyzed. Experiments were repeated three times. Scale bar in right panels of **a**, 25 μm; others, 50 μm.

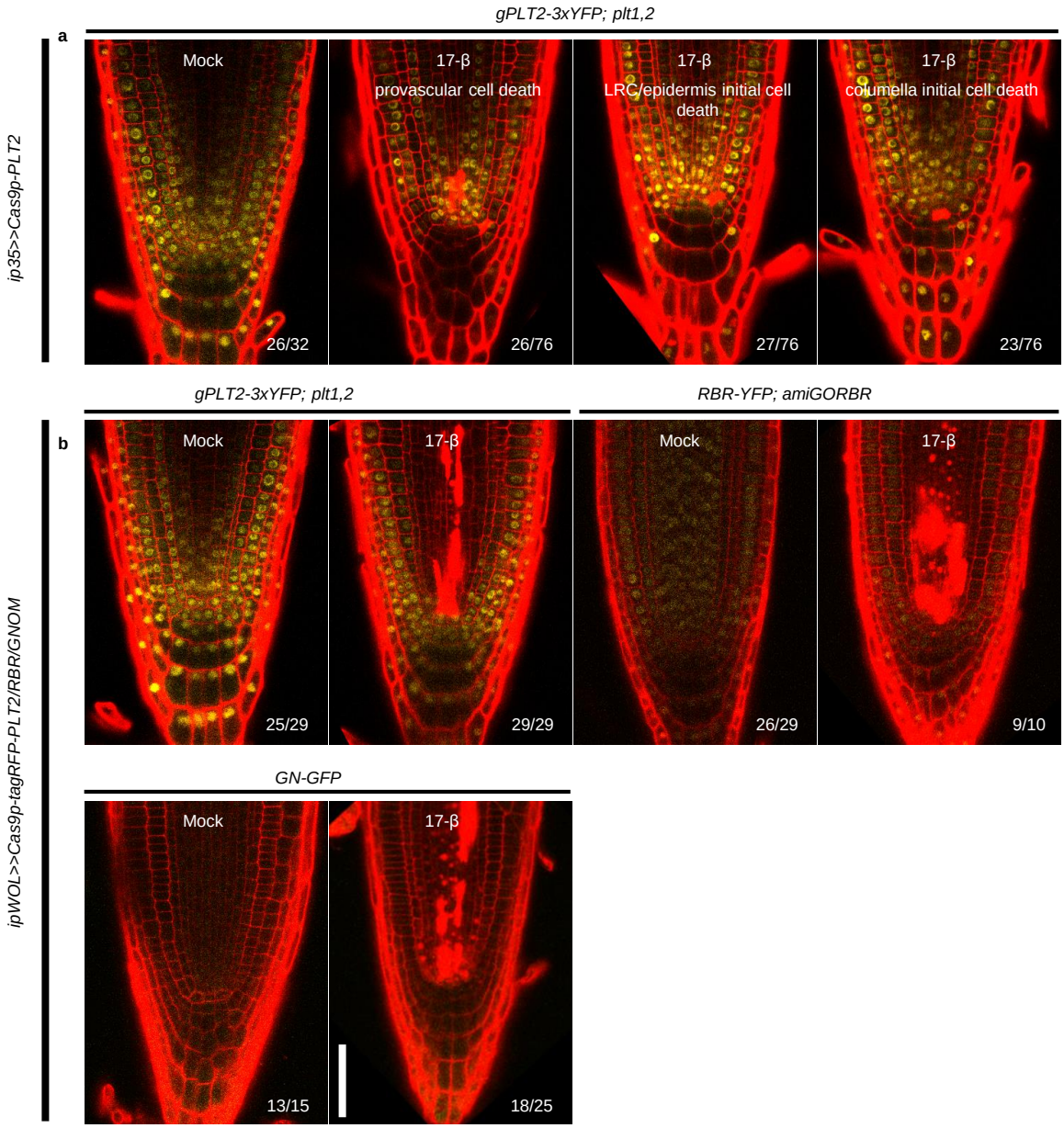

Extended Data Figure 8 Cas9p-mediated genome editing in proximal stem cells induces cell death.

(a) Stem cell death surrounding the QC was observed after one-day induction of *ip35S>>Cas9p-PLT2*. Based on cell types, the cell death response is classified into three categories: provascular cell death, LRC/epidermis initial cell death and columella initial cell death. Samples were counted twice if they had cell death in two different categories. **(b)** Cell death of provascular cells and early descendants was induced after one-day induction of *ipWOL>>Cas9p-tagRFP-PLT2/RBR/GNOM*. Cell walls are highlighted by propidium iodide (PI). Under PI detection settings, Cas9p-tagRFP is also visible. Numbers indicate the frequency of the observed phenotype in independent T1 samples analyzed. Experiments were repeated three times. Scale bars, 50 μm.

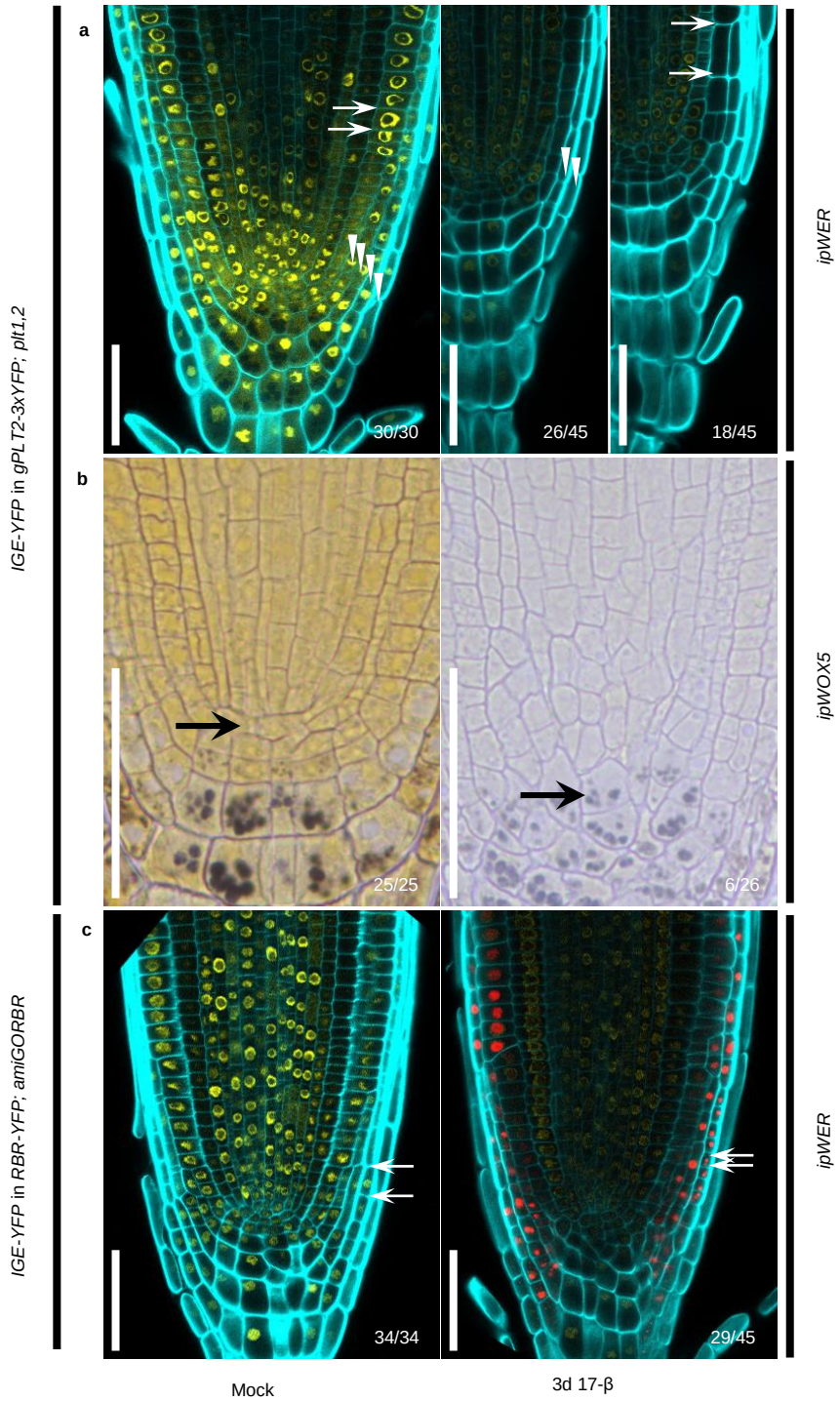

Extended Data Figure 9 A single IGE construct targeting a gene encoding a fluorescent reporter has the potential to disrupt different transgene targets.

(a) Editing *YFP* instead of *PLT2* in the *ipWER* expression region caused changes similar to direct *PLT2* editing. The RM had fewer LRC layers (white arrowheads), as well as premature expansion of epidermal cells and a broad, faint YFP signal. The Cas9p-tagRFP signal is frequently invisible. **(b)** Editing *YFP* led to QC (black arrow) differentiation at a lower frequency. **(c)** Targeting the *YFP* of RBR-YFP in the LRC led to LRC overproliferation, similar to editing RBR. However, the YFP signal outside *ipWER* expression region was also hampered by an unknown mechanism, unlike when editing *RBR*. White arrows mark the neighboring cell walls in **a** and **c**. The same construct was used in **a** and **c**. Cell walls are highlighted by calcofluor. Numbers indicate the frequency of the observed phenotype in independent T1 samples analyzed. Experiments were repeated three times. Scale bars, 50 μm.

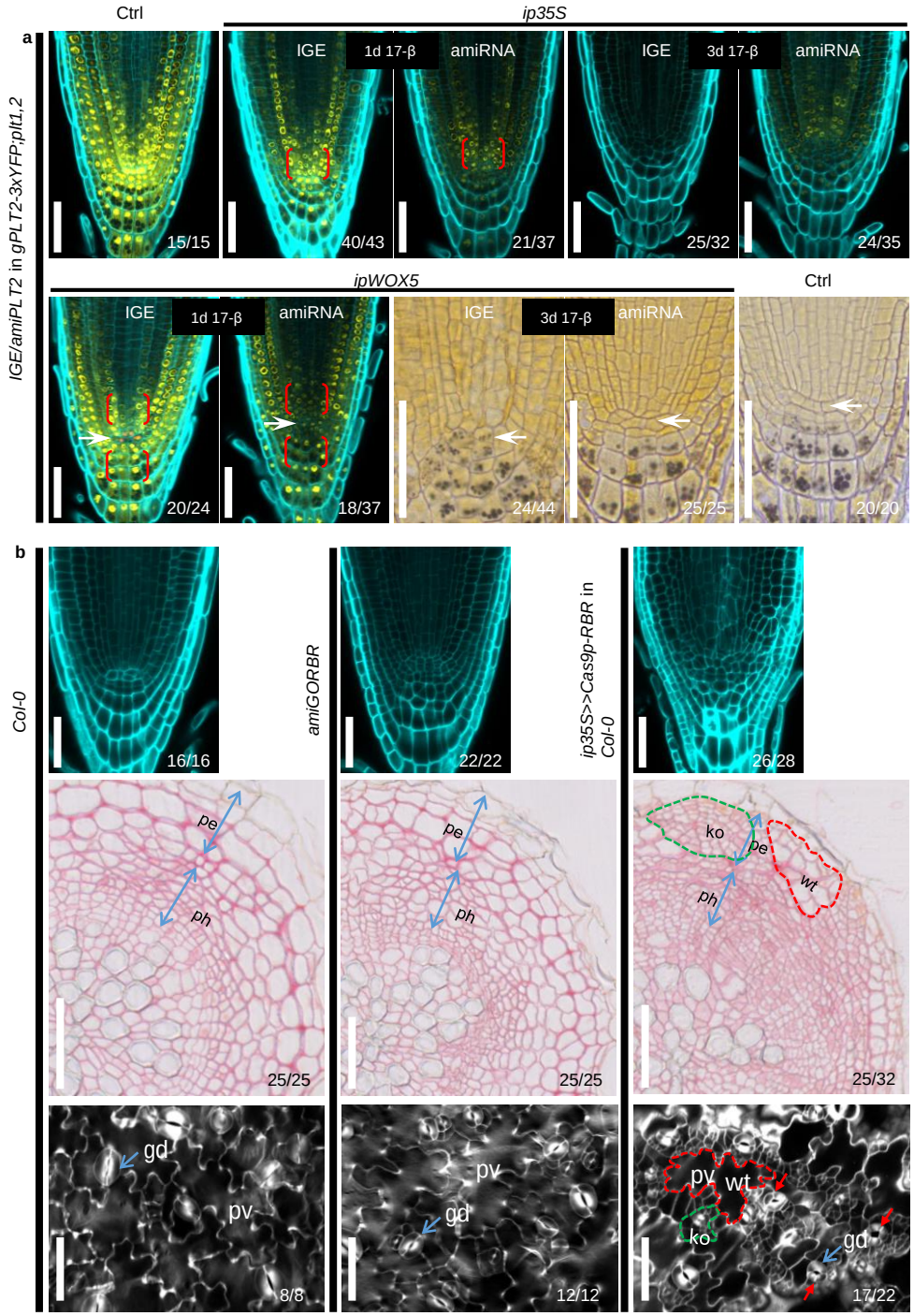

Extended Data Figure 10 Comparison of IGE system with inducible amiRNA.

(a) IGE-PLT2 displays more specific and stronger PLT2-3xYFP downregulation than amiPLT2. After a one-day induction, *ip35S>>amiPLT2-1* in *gPLT2-3xYFP*; *plt1,2* and *ipWOX5>>amiPLT2-1* in *gPLT2-3xYFP*; *plt1,2* showed a broader reduction of the YFP signal, particularly in the bracketed regions where no inducible promoter activity was found. Conversely, induced PLT2 editing caused very local loss of the YFP signal. After a three-day induction, the YFP signal is still visible in most of *ip35S>>amiPLT2-1* in *gPLT2-3xYFP*; *plt1,2* transformants but not in *ip35S>>Cas9p-PLT2* in *gPLT2-3xYFP*; *plt1,2* transformants. There was no QC differentiation in *ipWOX5>>amiPLT2-1* in *gPLT2-3xYFP*; *plt1,2* roots. Ctrl refers to 7-day (top panel) or 9-day (bottom panel) old *gPLT2-3xYFP*; *plt1,2*. White arrows mark the QC. (b) Comparison of the RM (top panel), root secondary growth (middle panel) and cotyledon epidermis (bottom panel) of Col-0, *35S:amiGORBR* and *ip35S>>Cas9p-RBR* in *Col-0*. Inducing RBR editing (germination on 17-β plates for 6 days (top panel), 20 days (middle panel) and 6 days (bottom panel)) resulted in more excessive cell divisions in the LRC than was seen in amiGORBR roots (top panel, germination and six days of growth on 17-β-free plates). Furthermore, RBR editing caused cell overproliferation in phloem (ph) cells and the periderm (pe) of root secondary tissues (middle panel) and pavement cells (pv) and guard cells (gd, blue arrows) of cotyledon epidermis (bottom panel), which was not observed in *amiGORBR* roots and cotyledons. The knockout (ko) sectors (green dotted line) were frequently accompanied by WT sectors (red dotted line), which can be regarded as an internal control. Red arrows mark guard cells divisions. Cell walls are marked by calcofluor. Numbers indicate the frequency of observed phenotype in independent samples analyzed. Experiments were repeated three times, except experiment on cotyledon epidermis phenotyping, which was repeated two times. Scale bars, 50 µm.

Supplementary Methods

To generate the *p221z-Cas9p-t35s* entry vector, first, *Cas9p* with two flanking nuclear localized signal (*NLS*) coding sequence and a *t35* terminator were amplified from vector *pYLCRISRPCas9P35S-B*[1] with chimeric primers which contained the *attB1/attB2* adaptor at the 5' end and a 3' end complementary to *NLS* and *t35s*, respectively. The resultant PCR fragment was gel-purified and then recombined with *pDONR 221* following the instructions of the Gateway BP Clonase II Enzyme mix (Invitrogen).

Site-directed mutations were introduced to two nuclease domains of Cas9p, RuvC1 and HNH (D10A, H840A)[2], respectively, to generate dCas9. To achieve this, a partial *Cas9p* fragment (61-2582, starting from ATG) was amplified with primers containing the desired mutations. The purified PCR fragment was then used as a mega-primer to amplify *p221z-Cas9p-t35s*. The resulting PCR product was digested by methylation-specific endonuclease Dpn I to remove the parental DNA template before transformation into competent *E.coli* DH5α cells. The presence of mutations in *p221z-dCas9p-t35s* was verified by Sanger sequencing.

To insert the *tagRFP* sequence between *Cas9p* and the 3' end of the *NLS* encoding sequence located in *p221z-Cas9p-t35s*, *tagRFP* was first amplified from the entry vector *p2R3a-tagRFP-OcsT*[3] with chimeric primers consisting of a 3' end of *tagRFP*-specific oligonucleotides and a 5' end of *Cas9p*/*NLS*-specific oligonucleotides complementary to the flanking sequence at the insertion point. The purified PCR fragment was then used as mega-primer in the subsequent Omega PCR step[4], which used *p221z-Cas9p-t35s* as the template. The PCR product was treated with Dpn I before transformation into competent *E.coli* DH5α cells. The insertion of *tagRFP* was verified by both enzyme digestion and Sanger sequencing.

To facilitate ligation of the sgRNA expression cassette (*pAtU3/6-sgRNA*) into a Gateway entry vector, the negative selection marker, a *ccdB* expression cassette flanked by two *Bsa I* sites, was amplified from *pYLCRISPRCas9P35S-B*[1] with primers containing *attB2/attB3* adaptors. After a BP

reaction with *pDONR P2R-P3z*, the reaction mixture was transformed into the ccdB-tolerant *E.coli* strain DB3.1. Colony PCR was performed to screen for positive colonies which had been transformed with recombined plasmids but not the empty *pDONR-P2R-P3z*. The presence of the *p2R3z-Bsa I-ccdB-Bsa I* entry vector was then further confirmed by enzyme digestion and Sanger sequencing.

To generate the *p221z-AtMIR390a* entry vector (Fig. 1b), a BP reaction was performed with *pDONR 221* and *pMDC123SB-AtMIR390a-B/c*[5] (Addgene ID: 51775). *pMDC123SB-AtMIR390a-B/c* contains *AtMIR390a* 5' end and *AtMIR390a* 3' end which were split by *Bsa I*-flanking *ccdB* expression modules. After transforming DB3.1, positive colonies were screened by colony PCR followed by enzyme digestion and sequencing. Two artificial microRNA against *PLT2* (*amiPLT2-1* and *amiPLT2-2*) were designed using http://p-sams.carringtonlab.org/. Annealed *amiPLT2* was ligated into *p221z-AtMIR390a* by a one-step reaction as previously described[5].

Tandem arrayed tRNA-sgRNA units have been exploited for multiplex genome editing by using the endogenous tRNA processing machinery[6], which precisely cuts tRNA precursors at both ends and releases free sgRNA after transcription. This strategy has been applied in a variety of plant species[6,7]. However, to date there are few reports of its application in *Arabidopsis*. We therefore investigated its feasibility in *Arabidopsis* genome editing and meanwhile tested its compatibility with our IGE system. To facilitate target sequence ligation, we first constructed a *p2R3z-AtU3b-tRNA-ccdB-sgRNA* entry vector (Fig. 1b). AtU3b, tRNA-1, tRNA-2 (tRNA was amplified in two separate fragments), the ccdB expression cassette (flanked by Bsa I), and the sgRNA scaffold were amplified with the indicated primer pairs. Both ends of each fragment contained primer-introduced sequences overlapping with the desired flanking fragments. In the overlapping PCR step, *attB2-AtU3b-F* and *attB3-sgRNA-R* were used as a primer pair to assemble these five purified PCR fragments, which were mixed as templates. Cloning this fused fragment into *pDONR P2R-P3z* was conducted as described above. To clone the first target sequence of *PLT2* into *p2R3z-AtU3b-tRNA-*

ccdB-sgRNA, two annealed primers with 4-nucleotide overhangs at the 5' ends and 20-nucleotide complementary target sequences were ligated into the entry vector in a one-step reaction as described previously[5]. In the *Arabidopsis* RM, we observed a decrease of the YFP signal in the region where the inducible promoter was active in most independent lines after a 1-day induction and finally a fully differentiated RM after a 10-day induction (Extended Data Fig. 4 and Supplementary Table 1), indicating that sgRNA against *PLT2* was disassociated from tRNA processing and guiding Cas9p to cleave *PLT2*. It has recently been reported that efficient genome editing could be achieved by fusing tRNA to a mutant sgRNA scaffold but not the wild type sgRNA scaffold in *Arabidopsis*[8]. However, in our hands wild type sgRNA scaffold and tRNA fusion worked well. We reasoned that the sgRNA promoter, Cas9 variant, sgRNA scaffold, target loci, and the tissue to be edited may all affect tRNA-sgRNA-mediated editing performance in *Arabidopsis*. Therefore a future comprehensive study of these variables may improve the utility of the tRNA processing system in *Arabidopsis*.

The red seed coat vector *pFRm43GW* was generated by modifying the *pHm43GW* destination vector[9], which was obtained from VIB (https://gateway.psb.ugent.be/). The *pHm43GW* vector was digested with PaeI (SphI) (ThermoFisher Scientific) to remove the hygromycin cassette. Using an In-Fusion HD Cloning (TaKaRa) kit, two fragments were cloned into the digested vector. The first fragment contained a *ccdB* cassette and recombination sites for MultiSite Gateway cloning, and it was amplified from *pHm43GW* using GAACCCTGTGGTTGGCATGCACATACAAATGGACGAACGGATAAA as a forward primer and ATACCTACATACACTTGAAGGGTACCCGGGGATCCTCTAGAGGG as a reverse primer. The second fragment contained the FastRed module, consisting of the *OLE1* promoter followed by *OLE1-tagRFP*, which was amplified from *pFAST-R01*[10] using CTTCAAGTGTATGTAGGTATAGTAACATG as a forward primer and

CGAATTGAATTATCAGCTTGCATGCAGGGTACCATCGTTCAAACATTTGGCAAT as a reverse primer.

We also provide another non-destructive fluorescent screening vector, the green seed coat vector *pFG7m34GW*. It was generated by cloning the FastGreen module into the *pP7m34GW* vector[9], which was obtained from VIB (https://gateway.psb.ugent.be/). The *pP7m34GW* vector was digested with SacI (ThermoFisher Scientific). Three fragments were cloned into the digested *pP7m34GW*. The first fragment contained the *OLE1* promoter followed by the *OLE1* genomic sequence and was amplified from *pFRm43GW* using CCATATGGGAGAGCTCCTTCAAGTGTATGTAGGTATAGT as a forward primer and GCCCTTGCTCACCATAGTAGTGTGCTGGCCACCACGAG as a reverse primer; the second fragment contained the *EGFP* encoding sequence and was amplified from the *pBGWFS7* vector[9] using ATGGTGAGCAAGGGCGAGGAGCTGT as a forward primer and ATCTATGTTACTAGATCACTTGTACAGCTCGTCCATGCC as a reverse primer; the third fragment contained the *nosT* terminator sequence and was amplified from the *p1R4-ML:XVE* vector[3] using TCTAGTAACATAGATGACACCGCGCG as a forward primer and TTAACGCCGAATTGAATTCGAGCTCCATCGTTCAAACAT as a reverse primer. All three fragments were combined together with the digested vector using In-Fusion HD Cloning.

Reference

1. Ma, X. *et al. Mol. Plant* **8**, 1274-1284 (2015).

2. Jinek, M. *et al. Science* **337**, 816-821 (2012).

3. Siligato, R. *et al. Plant Physiol.* **170**, 627-641 (2016).

4. Chen, L., Wang, F., Wang, X. & Liu, Y. G. *Plant Cell Physiol.* **54**, 634-642 (2013).

5. Carbonell, A. *et al. Plant Physiol.* **165**, 15-29 (2014).

6. Xie, K., Minkenberg, B. & Yang, Y. *Proc. Natl. Acad. Sci. USA* **112**, 3570-3575 (2015).

7. Jaganathan, D., Ramasamy, K., Sellamuthu, G., Jayabalan, S. & Venkataraman, G. *Front. Plant Sci.* **9**, 985 (2018).

8. Zhang, Q. *et al. Plant Mol. Biol.* **96**, 445-456 (2018).

9. Karimi, M., Inze, D. & Depicker, A. *Trends Plant Sci.* **7**, 193-195 (2002).

10. Shimada, T. L., Shimada, T. & Hara-Nishimura, I. *Plant J.* **61**, 519-528 (2010).

Supplementary Figure 1

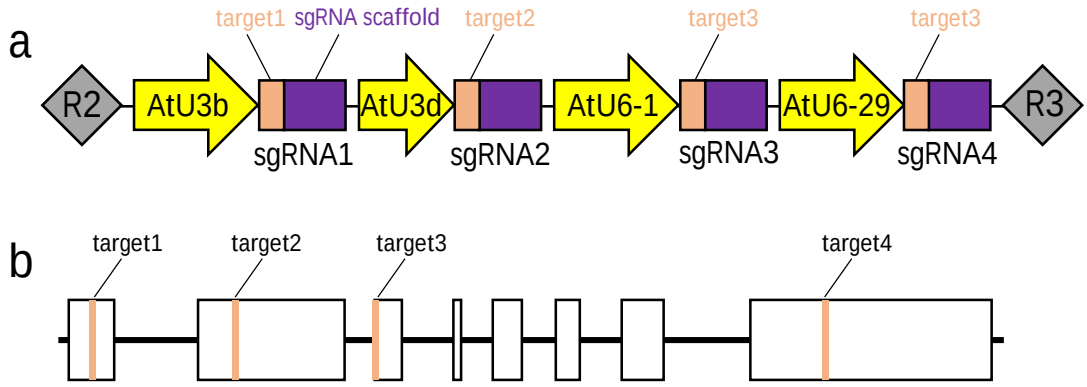

Supplementary Figure 1 IGE construct targeting *PLT2*.

(a) Tandem arrayed sgRNA expression cassettes. **(b)** The genomic structure of *PLT2*. Boxes indicate exons. Orange bars represent targets in *PLT2*.

Supplementary Figure 2

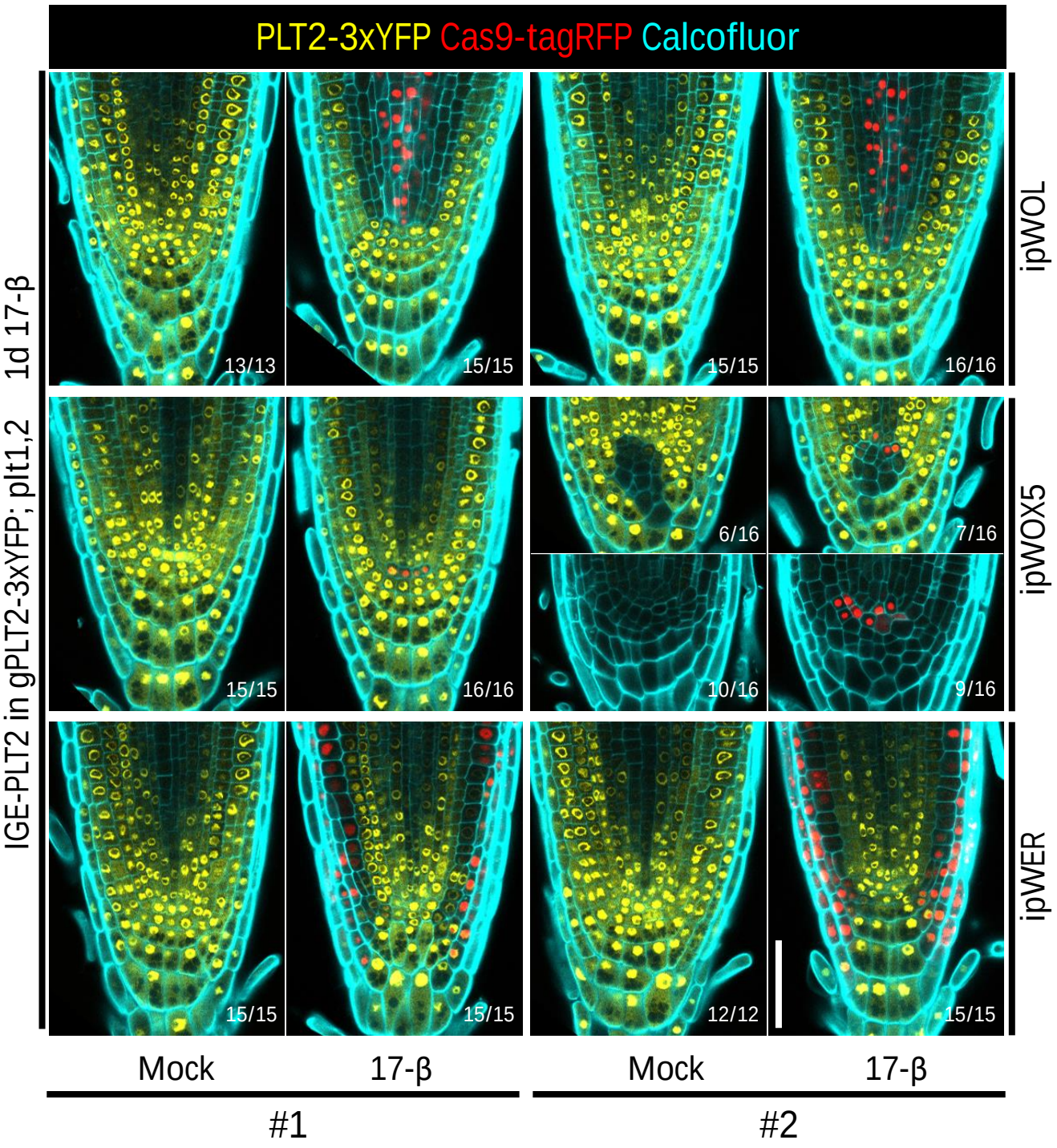

Supplementary Figure 2 IGE system-driven genome editing capability is inherited.

For each construct, two independent transgenic T2 lines were randomly selected and analyzed. Representative images are shown. Note that the second *ipWOX5>>Cas9p-tagRFP-PLT2* line was leaky: roots displayed a similar phenotype with/without induction. Cell walls are marked by calcofluor. Numbers represent the frequency of the observed phenotype in analyzed T2 samples. All experiments were repeated three times. Scale bar, 50 μm.

Supplementary Figure 3

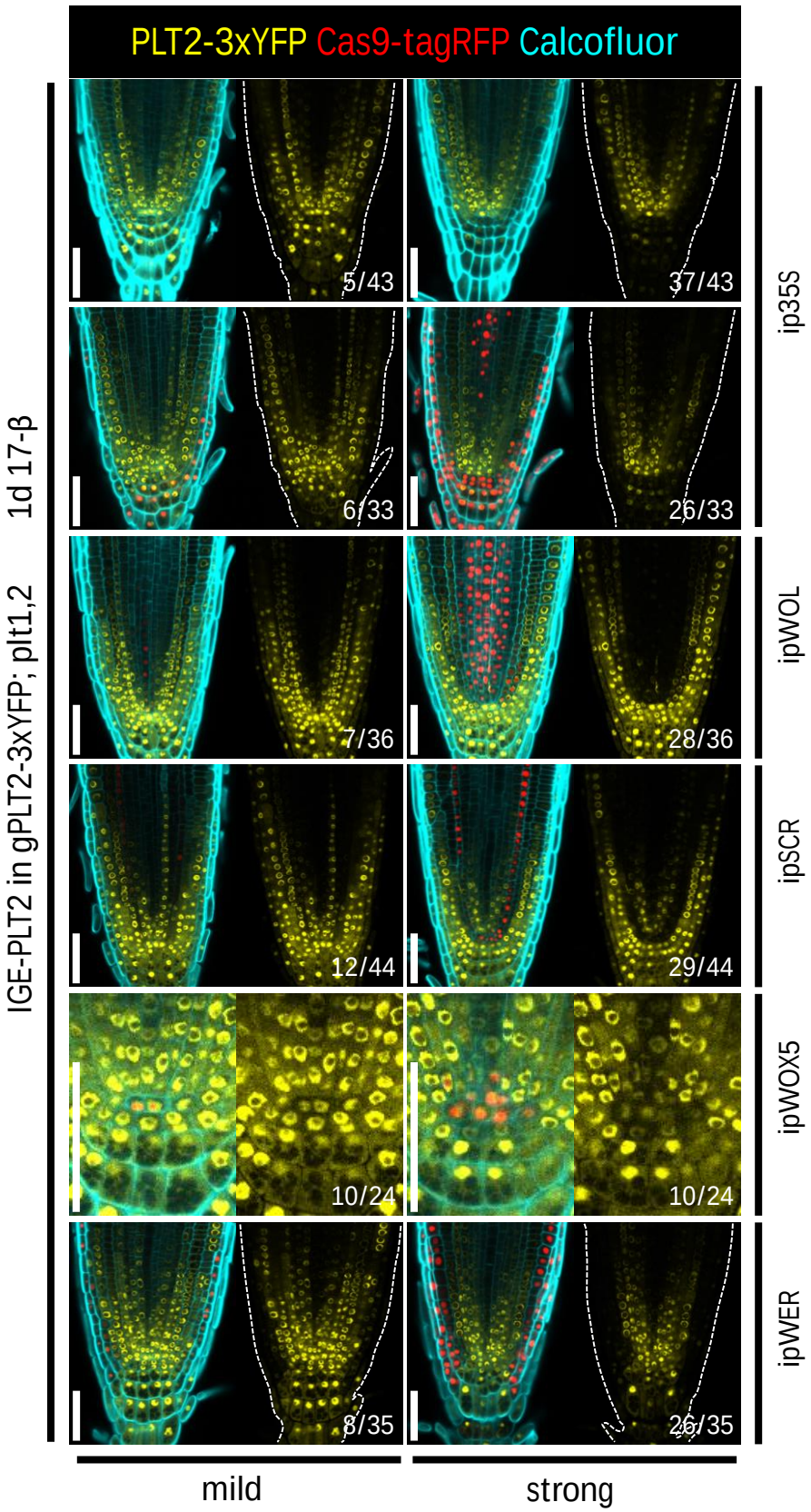

Supplementary Figure 3 IGE-mediated genome editing correlates with Cas9 expression.

After one day of induction, IGE performance on *PLT2* editing under different inducible promoters was classified into two categories. In the mild category, Cas9p/Cas9p-tagRFP expression tends to be weak and narrow, resulting in narrow domains of moderately decreased YFP signal. In the strong category, Cas9p-tagRFP expression was strong and broad, with strongly and broadly reduced YFP fluorescence. In the uppermost panel, Cas9p was used without a tag. White dotted lines mark the RM outlines. Cell walls are visualized by calcofluor. Numbers indicate the frequency of similar results in the T1 samples analyzed. All experiments were repeated at least three times. Scale bars, 50 μm.

Supplementary Figure 4

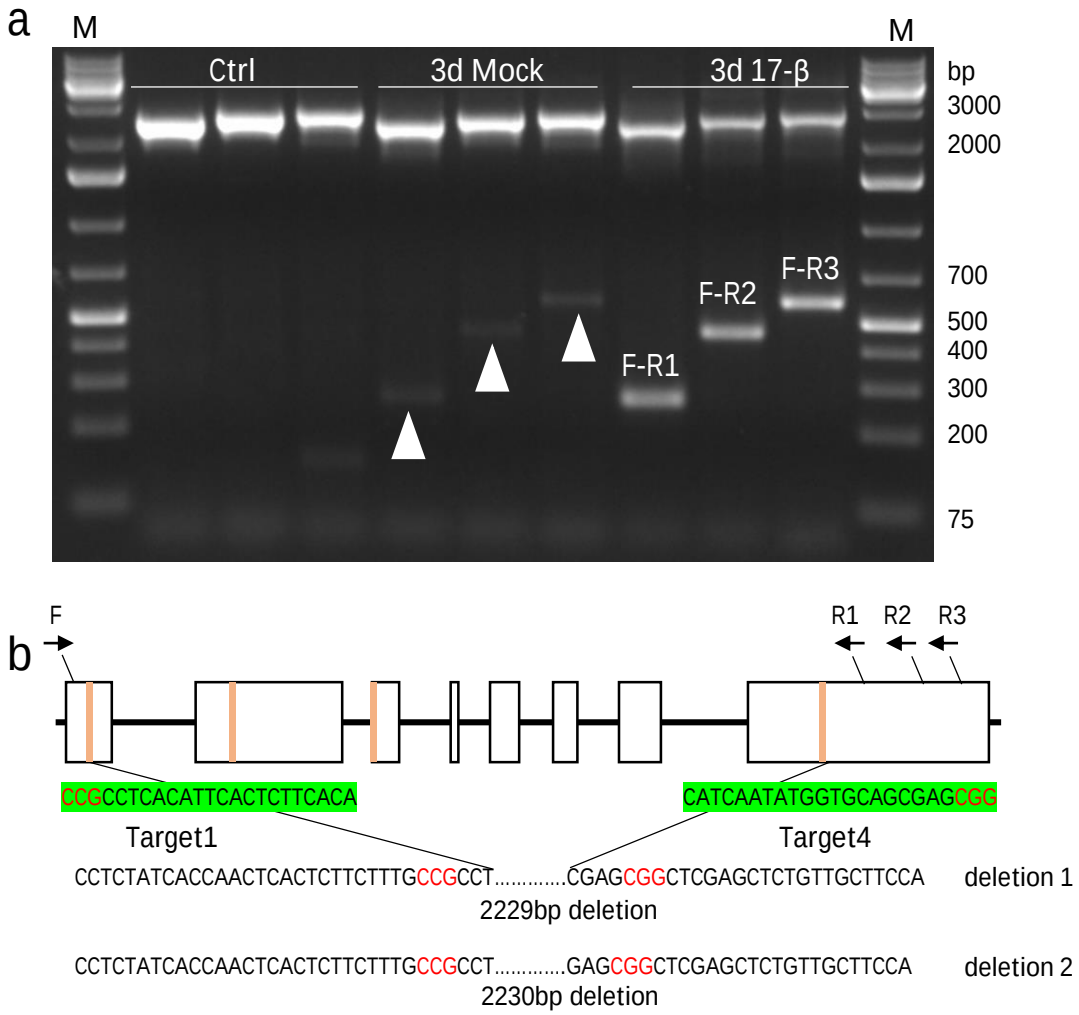

Supplementary Figure 4 PCR detection of IGE-mediated genome deletion.

(a) PCR detection of *PLT2* deletion in *ip35S>>Cas9p-PLT2* in *gPLT2-3xYFP*; *plt1,2* T1 seedlings after 3 days of treatment (in 6 day-old plants). Pooled DNA was isolated from 2cm root segments below the hypocotyl of 10 seedlings. Three primer pairs were used. There were no detectable truncated bands in 7-day old *gPLT2 3xYFP*; *plt1,2* (Ctrl), while weak truncated bands were detected in mock treated seedlings (white arrowhead), probably due to weak leakiness of *ip35S* in certain roots or cells. Note that although four sgRNAs were used to target *PLT2*, only one predominant truncated band was detected with each primer pair, corresponding to deletion between target1 and target4. Experiments were repeated three times. **(b)** Sequencing of truncated bands from primer pair F-R3 confirmed this deletion (letters in red represent protospacer adjacent motif, PAM). To determine the deletion types, the truncated band was not directly used for sequencing but cloned into *pDONR 221*. Two deletion types were found in 4 sequenced recombinant vectors. Black arrows represent relative positions of the forward and reverse primers.

Supplementary Figure 5

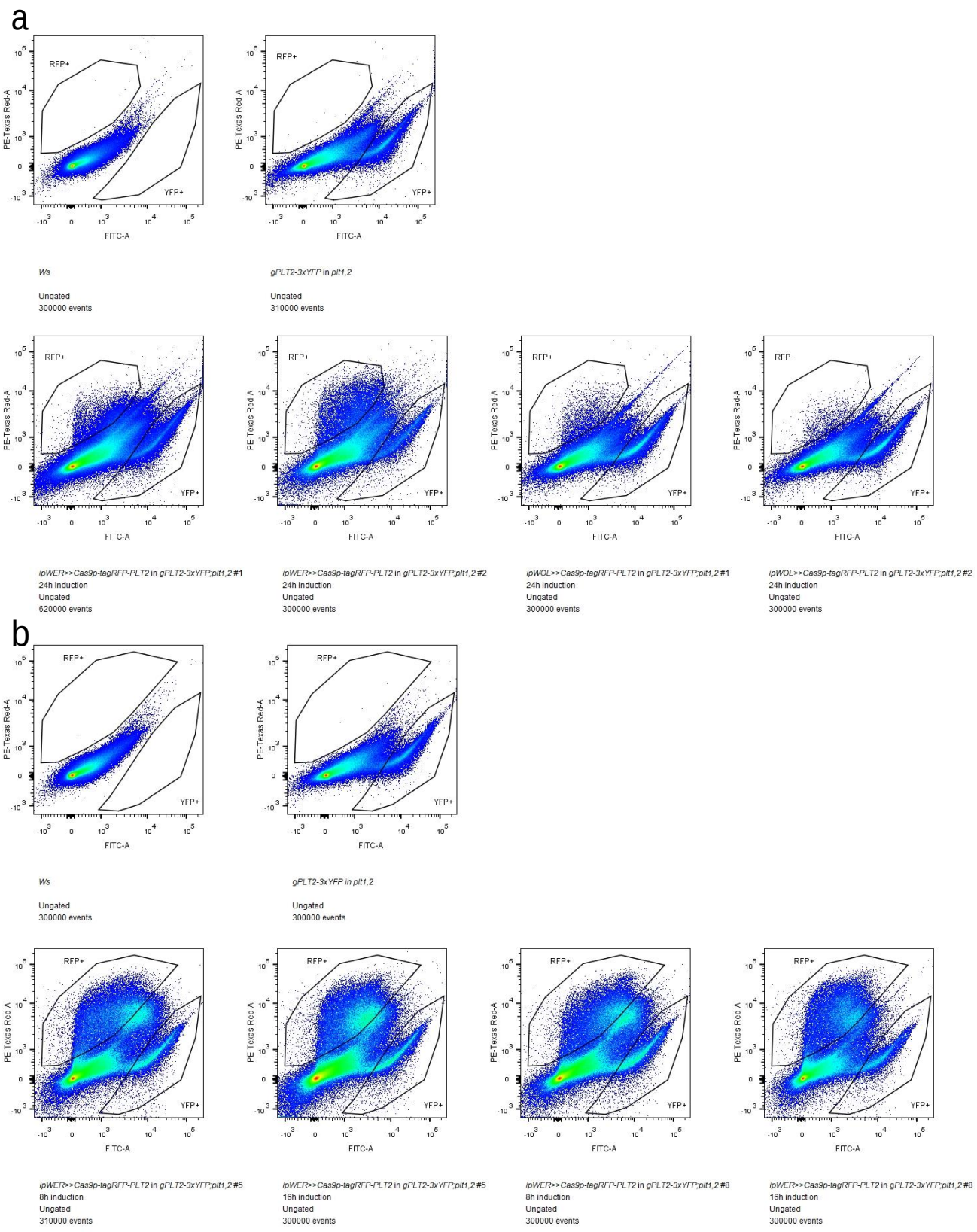

Supplementary Figure 5 Fluorescence-activated cell sorting of protoplasts obtained from IGE lines.

(**a**) FACS of protoplasts from T2 lines of *ipWER>>Cas9p-tagRFP-PLT2* in *gPLT2-3xYFP*; *plt1,2* and *ipWOL>>Cas9p-tagRFP-PLT2* in *gPLT2-3xYFP*; *plt1,2* after 24h induction. (**b**) FACS of protoplasts from time-course 17-β induced T2 lines of *ipWER>>Cas9p-tagRFP-PLT2* in *gPLT2-3xYFP*; *plt1,2*. Two independent transgenic lines of each construct were used for sorting. Each sample was sorted once.

Supplementary Figure 6

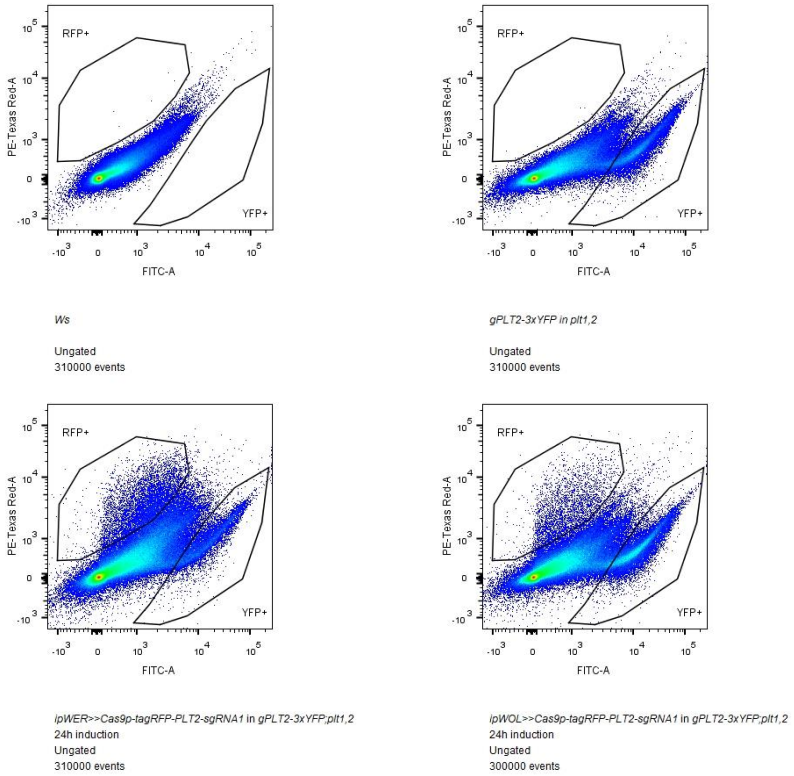

Supplementary Figure 6 Fluorescence-activated cell sorting of protoplasts obtained from IGE transformants containing one sgRNA.

FACS of protoplasts obtained from primary transformants (T1 generation) of *ipWER>>Cas9p-tagRFP-PLT2-sgRNA1* in *gPLT2-3xYFP*; *plt1,2* and *ipWOL>>Cas9p-tagRFP-PLT2-sgRNA1* in *gPLT2-3xYFP*; *plt1,2* after 24h induction. Sorting was performed once for each pooled T1 root material.

Supplementary Table 1 Quantification of fully differentiated root meristem (RM) after 10 days induction

1st BOX	2nd BOX	3rd BOX	Differentiated RM after 10d 17-β induction. Two repeats	
p1R4-35S:XVE	p221z-Cas9p-T35S	p2R3z-PLT2-AtU3b-sgRNA1	31/47 (66.0 %)	25/41 (61.0 %)
		p2R3z-PLT2-AtU3d-sgRNA1	17/32 (53,1 %)	20/48 (41,7 %)
		p2R3z-PLT2-AtU6-1-sgRNA1	0/29 (0.0 %)	0/43 (0.0 %)
		p2R3z-PLT2-AtU6-29-sgRNA1	15/23 (65.2 %)	22/34 (64.7 %)
		p2R3z-PLT2-AtU3b-tRNA-sgRNA1	20/34 (58.8 %)	25/31 (80.6 %)
		p2R3z-PLT2-AtU3b-sgRNA1+AtU3d-sgRNA2+AtU6-1-sgRNA3+AtU6-29-sgRNA4	17/32 (53.1 %)	25/35 (71.4 %)
	p221z-Cas9p-taqRFP-T35S	p2R3z-PLT2-AtU3b-sgRNA1	21/32 (65.6 %)	23/39 (59.0 %)
	p221z-dCas9p-T35S	p2R3z-PLT2-AtU3b-sgRNA1+AtU3d-sgRNA2+AtU6-1-sgRNA3+AtU6-29-sgRNA4	0/32 (0.0 %)	0/41 (0.0 %)
	p221z-AtMIR390-PLT2-1	p2R3z-nosT2	0/29 (0.0 %)	0/32 (0.0 %)
	p221z-AtMIR390-PLT2-2	p2R3z-nosT2	0/24 (0.0 %)	0/37 (0.0 %)

Supplementary Table 2 Primer used in this study

Primer name	sequence(5'-3')	purpose
attB1-Cas9p-T35s-F	GGGGACAAGTTTGTACAAAAAAGCAGGCTCGATGGCTCCTAAGAAGAAGCG	For cloning Cas9p with T35s terminator into 2nd BOX
attB2-Cas9p-T35s-R	GGGGACCACTTTGTACAAGAAAGCTGGGTGGTCACTGGATTTTGGTTTTAGG	
attB2-ccdB-F	GGGGACAGCTTTCTTGTACAAAGTGGAACTCGAGAGACCTCTGAAGTGG	For cloning Bsa I-ccdB-Bsa I into 3 box
attB3-ccdB-R	GGGGACAACTTTGTATAATAAAGTTGAACCGCGAGACCCACGCTCAC	
PLT2-TG1-gRT#+	TGTGAAGAGTGAATGTGAGGGTTTTAGAGCTAGAAAT	For cloning 4 sgRNA expression cassettes targeting PLT2
PLT2-TG1-AtU3bT#-	CCTCACATTCACTCTTCACATGACCAATGTTGCTCC	
PLT2-TG2-gRT#+	ATAAGGTACGAGGTTGTGATGTTTTAGAGCTAGAAAT	
PLT2-TG2-AtU3dT#-	ATCACAACCTCGTACCTTATTGACCAATGGTGCTTTG	
PLT2-TG3-gRT#+	TTAGATAACTAACTACGAGAGTTTTAGAGCTAGAAAT	
PLT2-TG3-AtU6-1T#-	TCTCGTAGTTAGTTATCTAACAATCACTACTTCGTCT	
PLT2-TG4-gRT#+	CATCAATATGGTGCAGCGAGGTTTTAGAGCTAGAAAT	
PLT2-TG4-AtU6-29T#-	CTCGCTGCACCATATTGATGCAATCTCTTAGTCGACT	
dCas9p-D10A-F	TACTCCATCGGCCTCgcgATCGGCACCAACAGC	dCas9 cloning
dCas9p-H840A-R	GACTGAGGAACAATcgcGTCGACGTCGTAGT	
attB1-gPLT2-F	GGGGACAAGTTTGTACAAAAAAGCAGGCTCGATGAATTCTAACAACTGGCTC	PCR detection of PLT2 deletion from genome, and subsequent cloning into pDONR221z for sequencing
attB2-gPLT2-R1	GGGGACCACTTTGTACAAGAAAGCTGGGTGGAATCATGATACTGAGAGAT	
attB2-gPLT2-R2	GGGGACCACTTTGTACAAGAAAGCTGGGTGGAGCTTGACCCAATACCAAT	
attB2-gPLT2-R3	GGGGACCACTTTGTACAAGAAAGCTGGGTGGATCCTTGAGCAGACTCTCC	
amiPLT2-1-F	TGTATGATGATCCCCCGATTTGCTGATGATGATCACATTCGTTATCTATTTTTTCAGCAAATCGTGGGATCATCA	amiPLT2-1 cloning
amiPLT2-1-R	AATGTGATGATCCCACGATTTGCTGAAAAAATAGATAACGAATGTGATCATCATCAGCAAATCGGGGGATCATCA	
amiPLT2-2-F	TGTATGATCGGTGTGATGATCCCCGATGATGATCACATTCGTTATCTATTTTTTCGGGGATCATAACACCGATCA	amiPLT2-2 cloning
amiPLT2-2-R	AATGTGATCGGTGTTATGATCCCCGAAAAAATAGATAACGAATGTGATCATCATCGGGGATCATCACACCGATCA	
PLT2-TG1-AtU3dT#-	CCTCACATTCACTCTTCACATGACCAATGGTGCTTTG	sgRNA promoter comparison
PLT2-TG1-AtU6-1T#-	CCTCACATTCACTCTTCACACAATCACTACTTCGTCT	
PLT2-TG1-AtU6-29T#-	CCTCACATTCACTCTTCACACAATCTCTTAGTCGACT	
YFP-gRT	CCCATCCTGGTCGAGCTGGAGTTTTAGAGCTAGAAAT	YFP targeting
AtU3b-YFP	TCCAGCTCGACCAGGATGGGTGACCAATGTTGCTCC	
RBR-TG1-gRT#+	TCAGCAAGCATGTCTAACATGTTTTAGAGCTAGAAAT	For cloning 4 sgRNA expression cassettes targeting RBR
RBR-TG1-AtU3bT#	ATGTTAGACATGCTTGCTGATGACCAATGTTGCTCC	
RBR-TG2-gRT#+	GTCAAGGCTGGATCTGTACTGTTTTAGAGCTAGAAAT	
RBR-TG2-AtU3dT#	AGTACAGATCCAGCCTTGACTGACCAATGGTGCTTTG	
RBR-TG3-gRT#+	TATCCTCAACTCATCTTCTGGTTTTAGAGCTAGAAAT	
RBR-TG3-AtU6-1T#	CAGAAGATGAGTTGAGGATACAATCACTACTTCGTCT	
RBR-TG4-gRT#+	TATGACAGTCCTGAGCCACTGTTTTAGAGCTAGAAAT	
RBR-TG4-AtU6-29T#	AGTGGCTCAGGACTGTCATACAATCTCTTAGTCGACT	
GNOM-TG1-gRT#+	ACTACACTTGTCAACAGAGCGTTTTAGAGCTAGAAAT	For cloning 4 sgRNA expression cassettes targeting GNOM
GNOM-TG1-AtU3bT#	GCTCTGTTGACAAGTGTAGTTGACCAATGTTGCTCC	
GNOM-TG2-gRT#+	TTGATGGATGATGGACCAGTGTTTTAGAGCTAGAAAT	
GNOM-TG2-AtU3dT#	ACTGGTCCATCATCCATCAATGACCAATGGTGCTTTG	
GNOM-TG3-gRT#+	GTGTACTCATCAAGATGGACGTTTTAGAGCTAGAAAT	
GNOM-TG3-AtU6-1T#	GTCCATCTTGATGAGTACACCAATCACTACTTCGTCT	
GNOM-TG4-gRT#+	TCAGCTCATCTACAGTCAATGTTTTAGAGCTAGAAAT	
GNOM-TG4-AtU6-29T#	ATTGACTGTAGATGAGCTGACAATCTCTTAGTCGACT	

attB2-AtU3b-F	GGGGACAGCTTTCTTGTACAAAGTGGAATTTACTTTAAATTTTTTCTTAT	Generating p2R3z-AtU3b-tRNA-ccdB-gRNA entry clone
tRNA-AtU3b-R	ACCACTAGACCACTGGTGCTTTGTTTGACCAATGTTGCTCCCTCAGTGTT	
AtU3b-tRNA-F	TAACACTGAGGGAGCAACATTGGTCAAACAAAGCACCAGTGGTCTA	
tRNA-R	CCGTGGCAGGGTACTATTCTACCACTAGACCACTGGTGCTTTGTT	
tRNA-F	AGAATAGTACCCTGCCACGGTACAGACCCGGGTTCGATTCCCGGCT	
ccdB-tRNA-R	TGAATCGGCCACTTCAGAGGTCTCTTGCACCAGCCGGGAATCGAACCCGGG	
tRNA-ccdB-F	CCCGGGTTCGATTCCCGGCTGGTGCAAGAGACCTCTGAAGTGGCCGATTCA	
ccdB-sgRNA-R	AACTTGCTATTTCTAGCTCTAAAACCGAGACCCACGCTCACCCGCCGCGC	
ccdB-sgRNA-F	GCGCGGCGGGTGAGCGTGGGTCTCGGTTTTAGAGCTAGAAATAGCAAGTT	
attB3-sgRNA-R	GGGGACAACTTTGTATAATAAAGTTGAAAAAAAAAAGCACCGACTCGGTGCCA	
BSAI-PLT2-TG1-F	TGCATGTGAAGAGTGAATGTGAGG	For cloning PLT2 target 1 into 2R3z-AtU3b-tRNA-ccdB-gRNA entry clone
BSAI-PLT2-TG1-R	AAACCCTCACATTCACTCTTCACA	
Cas9-RFP-F	CGTATCGACCTTTCCCAGCTTGGTGGTGATATGAGCGAGCTGATTAAGGA	For making p221z-Cas9p-tagRFP entry clone
NLS-RFP-R	TCCGGCCTTTTTGGTGGCAGCAGGACGCTTCTTGTGCCCCAGTTTGCTAG	
PLT2-TG1-F1	GCTTTGATTCCAAGAAAAGGG	TIDE analysis or amplicon sequencing
PLT2-TIDE-TG1-R1	CATGTGCAATGATGCTTTCGA	
PLT2-TIDE-TG1-R2	GTGGATTGATCATATTCCATC	
PLT2-TIDE-TG2-F	GATGGAATATGATCAATCCAC	
PLT2-TIDE-TG2-R	CTACCGGTCCATCTATGTCT	
PLT2-TIDE-TG3-F	GTGGGTATGACAAAGAAGAG	
PLT2-TIDE-TG3-R	CTTACTGAATGTTCCCAAGTAG	
PLT2-TIDE-TG4-F	GCACGGAGGAAGAAGCAGCAG	
PLT2-TIDE-TG4-R	GAGCTTGACCCAATACCAAT	
PLT2-TG1-F2	ATGAATTCTAACAACTGGCTCG	Amplicon sequecing
PLT2-TG1-R	ATGTCTTAATATTTGAACCCTTCG	
PLT2-qPCR-F	TGTACAAAAAAGCAGGCTTCATG	Quantification of genome deletion of transgenic PLT2
PLT2-qPCR-R	GTTGACCAAACCTAGATTGAAATG	

Underlined sequences indicate Gateway adaptors. Sequence in red represent the target sequence in the gene.

Supplementary Table 3 Constructs generated in this study

Expression vector name	1st BOX	2nd BOX	3rd BOX	Destination vector
35S:XVE>>Cas9p-PLT2-AtU3b-sgRNA1	p1R4-35S:XVE	p221z-Cas9p-T35S	p2R3z-PLT2-AtU3b-sgRNA1	pBm43GW
35S:XVE>>Cas9p-PLT2-AtU3d-sgRNA1	p1R4-35S:XVE	p221z-Cas9p-T35S	p2R3z-PLT2-AtU3d-sgRNA1	pBm43GW
35S:XVE>>Cas9p-PLT2-AtU6-1-sgRNA1	p1R4-35S:XVE	p221z-Cas9p-T35S	p2R3z-PLT2-AtU6-1-sgRNA1	pBm43GW
35S:XVE>>Cas9p-PLT2-AtU6-29-sgRNA1	p1R4-35S:XVE	p221z-Cas9p-T35S	p2R3z-PLT2-AtU6-29-sgRNA1	pBm43GW
35S:XVE>>Cas9p-PLT2-AtU3b-tRNA-sgRNA1	p1R4-35S:XVE	p221z-Cas9p-T35S	p2R3z-PLT2-AtU3b-tRNA-sgRNA1	pFRm43GW
35S:XVE>>Cas9p-PLT2-sgRNA1-4	p1R4-35S:XVE	p221z-Cas9p-T35S	p2R3z-PLT2-AtU3b-sgRNA1+AtU3d-sgRNA2+AtU6-1-sgRNA3+AtU6-29-sgRNA4	pBm43GW
35S:XVE>>dCas9p-PLT2-sgRNA1-4	p1R4-35S:XVE	p221z-dCas9p-T35S	p2R3z-PLT2-AtU3b-sgRNA1+AtU3d-sgRNA2+AtU6-1-sgRNA3+AtU6-29-sgRNA4	pBm43GW
35S:XVE>>Cas9p-tagRFP-PLT2-AtU3b-sgRNA1	p1R4-35S:XVE	p221z-Cas9p-tagRFP-T35S	p2R3z-PLT2-AtU3b-sgRNA1	pBm43GW
35S:XVE>>AtMIR390-PLT2-1-nosT2	p1R4-35S:XVE	p221z-AtMIR390-PLT2-1	nosT2	pFRm43GW
35S:XVE>>AtMIR390-PLT2-2-nosT2	p1R4-35S:XVE	p221z-AtMIR390-PLT2-2	nosT2	pFRm43GW
pWOX5:XVE>>AtMIR390-PLT2-1-nosT2	p1R4-pWOX5:XVE	p221z-AtMIR390-PLT2-1	nosT2	pFRm43GW
pWER:XVE>>Cas9p-tagRFP-PLT2-sgRNA1-4	p1R4-pWER:XVE	p221z-Cas9p-tagRFP-T35S	p2R3z-PLT2-AtU3b-sgRNA1+AtU3d-sgRNA2+AtU6-1-sgRNA3+AtU6-29-sgRNA4	pBm43GW
pWOX5:XVE>>Cas9p-tagRFP-PLT2-sgRNA1-4	p1R4-pWOX5:XVE	p221z-Cas9p-tagRFP-T35S	p2R3z-PLT2-AtU3b-sgRNA1+AtU3d-sgRNA2+AtU6-1-sgRNA3+AtU6-29-sgRNA4	pBm43GW
pSCR:XVE>>Cas9p-tagRFP-PLT2-sgRNA1-4	p1R4-pSCR:XVE	p221z-Cas9p-tagRFP-T35S	p2R3z-PLT2-AtU3b-sgRNA1+AtU3d-sgRNA2+AtU6-1-sgRNA3+AtU6-29-sgRNA4	pBm43GW
pWOL:XVE>>Cas9p-tagRFP-PLT2-sgRNA1-4	p1R4-pWOL:XVE	p221z-Cas9p-tagRFP-T35S	p2R3z-PLT2-AtU3b-sgRNA1+AtU3d-sgRNA2+AtU6-1-sgRNA3+AtU6-29-sgRNA4	pBm43GW
pWER:XVE>>Cas9p-taRFP-RBR-sRNA1-4	p1R4-pWER:XVE	p221z-Cas9p-tagRFP-T35S	p2R3z-RBR-AtU3b-sgRNA1+AtU3d-sgRNA2+AtU6-1-sgRNA3+AtU6-29-sgRNA4	pFRm43GW
pWOX5:XVE>>Cas9p-taRFP-RBR-sRNA1-4	p1R4-pWOX5:XVE	p221z-Cas9p-tagRFP-T35S	p2R3z-RBR-AtU3b-sgRNA1+AtU3d-sgRNA2+AtU6-1-sgRNA3+AtU6-29-sgRNA4	pFRm43GW
pSCR:XVE>>Cas9p-taRFP-RBR-sRNA1-4	p1R4-pSCR:XVE	p221z-Cas9p-tagRFP-T35S	p2R3z-RBR-AtU3b-sgRNA1+AtU3d-sgRNA2+AtU6-1-sgRNA3+AtU6-29-sgRNA4	pFRm43GW
pWOL:XVE>>Cas9p-taRFP-RBR-sRNA1-4	p1R4-pWOL:XVE	p221z-Cas9p-tagRFP-T35S	p2R3z-RBR-AtU3b-sgRNA1+AtU3d-sgRNA2+AtU6-1-sgRNA3+AtU6-29-sgRNA4	pFRm43GW
35S:XVE>>Cas9p-RBR-sgRNA1-4	p1R4-35S:XVE	p221z-Cas9p-T35S	p2R3z-RBR-AtU3b-sgRNA1+AtU3d-sgRNA2+AtU6-1-sgRNA3+AtU6-29-sgRNA4	pFRm43GW
pWER:XVE>>Cas9p-tagRFP-AtU3b-YFP-sgRNA	p1R4-pWER:XVE	p221z-Cas9p-tagRFP-T35S	2R3z-YFP-AtU3b-sgRNA	pFRm43GW
pWOX5:XVE>>Cas9p-tagRFP-AtU3b-YFP-sgRNA	p1R4-pWOX5:XVE	p221z-Cas9p-tagRFP-T35S	2R3z-YFP-AtU3b-sgRNA	pFRm43GW
pWOL:XVE>>Cas9p-tagRFP-GNOM-sgRNA1-4	p1R4-pWOL:XVE	p221z-Cas9p-tagRFP-T35S	p2R3z-GNOM-AtU3b-sgRNA1+AtU3d-sgRNA2+AtU6-1-sgRNA3+AtU6-29-sgRNA4	pFRm43GW

Expression vector name	1st BOX	2nd BOX	3rd BOX	Destination vector
pWER:XVE>>Cas9p-tagRFP-PLT2-sgRNA1	p1R4-pWER:XVE	p221z-Cas9p-tagRFP-T35S	p2R3z-PLT2-AtU3b-sgRNA1	pFRm43GW
pWOL:XVE>>Cas9p-tagRFP-PLT2-sgRNA1	p1R4-pWOL:XVE	p221z-Cas9p-tagRFP-T35S	p2R3z-PLT2-AtU3b-sgRNA1	pFRm43GW